Biochemical and Biophysical Research Communications 448 (2014) 175–181

Contents lists available at ScienceDirect

Biochemical and Biophysical Research Communications

journal homepage: www.elsevier.com/locate/ybbrc

Functional analysis of iPSC-derived myocytes from a patient with carnitine palmitoyltransferase II deficiency

Tetsuhiko Yasuno [a,*], Kenji Osafune [b], Hidetoshi Sakurai [b], Isao Asaka [b], Akihito Tanaka [b], Seiji Yamaguchi [c], Kenji Yamada [c], Hirofumi Hitomi [b], Sayaka Arai [b], Yuko Kurose [b], Yasuki Higaki [d], Mizuki Sudo [d], Soichi Ando [d], Hitoshi Nakashima [a], Takao Saito [a,e], Hidetoshi Kaneoka [a,f]

[a] Division of Nephrology and Rheumatology, Department of Internal Medicine, Fukuoka University School of Medicine, Fukuoka, Japan
[b] Center for iPS Cell Research and Application (CiRA), Kyoto University, Kyoto, Japan
[c] Department of Pediatrics, Shimane University School of Medicine, Izumo, Shimane, Japan
[d] Faculty of Sports and Health Science, Fukuoka University, Japan
[e] General Medical Research Center, Fukuoka University School of Medicine, Japan
[f] Division of Medical Sciences, Fukuoka University School of Nursing, Japan

ARTICLE INFO

Article history:
Received 13 April 2014
Available online 26 April 2014

Keywords:
Carnitine palmitoyltransferase II deficiency
iPSC
Disease modeling
Rhabdomyolysis
Bezafibrate

ABSTRACT

Introduction: Carnitine palmitoyltransferase II (CPT II) deficiency is an inherited disorder involving β-oxidation of long-chain fatty acids (FAO), which leads to rhabdomyolysis and subsequent acute renal failure. The detailed mechanisms of disease pathogenesis remain unknown; however, the availability of relevant human cell types for investigation, such as skeletal muscle cells, is limited, and the development of novel disease models is required.

Methods: We generated human induced pluripotent stem cells (hiPSCs) from skin fibroblasts of a Japanese patient with CPT II deficiency. Mature myocytes were differentiated from the patient-derived hiPSCs by introducing myogenic differentiation 1 (*MYOD1*), the master transcriptional regulator of myocyte differentiation. Using an *in vitro* acylcarnitine profiling assay, we investigated the effects of a hypolipidemic drug, bezafibrate, and heat stress on mitochondrial FAO in CPT II-deficient myocytes and controls.

Results: CPT II-deficient myocytes accumulated more palmitoylcarnitine (C16) than did control myocytes. Heat stress, induced by incubation at 38 °C, leads to a robust increase of C16 in CPT II-deficient myocytes, but not in controls. Bezafibrate reduced the amount of C16 in control and CPT II-deficient myocytes.

Discussion: In this study, we induced differentiation of CPT II-deficient hiPSCs into mature myocytes in a highly efficient and reproducible manner and recapitulated some aspects of the disease phenotypes of CPT II deficiency in the myocyte disease models. This approach addresses the challenges of modeling the abnormality of FAO in CPT II deficiency using iPSC technology and has the potential to revolutionize translational research in this field.

1. Introduction

β-Oxidation of long-chain fatty acids (LCFA) occurs in the mitochondria with the activity of carnitine palmitoyltransferase II (CPT II; EC2.3.1.21), carnitine-acylcarnitine translocase (CACT), CPT I, and acyl-coenzyme A (CoA) synthetase. These enzymes mediate LCFA transport from the cytosol into the mitochondria. In response to conditions with a high-energy demand, such as intensive exercise, severe infection, and fasting, LCFA transfer is promptly activated [1–4]. *CPT2* maps to chromosome 1p32, spans 20 kb, contains five exons, and encodes the CPT II enzyme. Defects in CPT II enzymatic activity are classified into three clinical categories in humans: lethal neonatal (MIM #608836), severe infantile (MIM #600649), and mild adult-onset (MIM #255110) types. Due to the low enzymatic activity of CPT II, the neonatal and infantile forms result in liver failure, hypoketotic hypoglycemia, and cardiomegaly. The neonatal form causes death within several months. The infantile form has been implicated in cases of sudden infant death syndrome. On the other hand, the adult-onset type

* Corresponding author. Address: Division of Nephrology and Rheumatology, Department of Internal Medicine, Fukuoka University School of Medicine, 7-45-1 Nanakuma, Jonan-ku, Fukuoka, Fukuoka 814-0180, Japan. Fax: +81 92 873 8008.
E-mail address: yasuno9584@fukuoka-u.ac.jp (T. Yasuno).

http://dx.doi.org/10.1016/j.bbrc.2014.04.084
0006-291X/

manifests as recurrent myalgia (muscle pain), rhabdomyolysis, and myoglobinuria, which can cause acute renal failure. CPT II deficiency is generally considered an autosomal recessive disease; however, many cases of symptomatic carriers have been reported [5]. Individuals who carry a *CPT2* mutation [6–9] may develop the clinical features of CPT II deficiency when treated with medications that affect the activity of the remaining wild-type CPT II enzyme.

In this study, we successfully derived human induced pluripotent stem cells (hiPSCs) from a patient with CPT II deficiency, differentiated them into a mature myocyte lineage within 2 weeks in a highly efficient and reproducible manner, and recapitulated some of the disease phenotypes associated with CPT II deficiency. We discuss the opportunities to use iPSC technology for modeling defects in FAO and for evaluating therapeutic regimens for CPT II deficiency.

2. Patient and methods

2.1. Patient

The subject of the current study was a 24-year-old Japanese man whose genetic and clinical presentation has already been described [10]. The patient suffered from acute renal failure induced by rhabdomyolysis and was diagnosed as having adult-onset CPT II deficiency. Skin biopsy samples were obtained from the patient with his written informed consent. This study was approved by the Ethics Committee on hereditary disease, Research of the Graduate School of Medical Sciences, Fukuoka University, and by the Ethics Committee of Kyoto University. The dermal fibroblasts were expanded from skin biopsy explants in Dulbecco's modified Eagle's medium (DMEM; Nacalai Tesque, Kyoto, Japan) supplemented with 10% fetal bovine serum (Japan Bioserum, Hiroshima, Japan). Control iPSCs (201B7) were previously established from the facial dermis of a 36-year-old Caucasian woman at the Center for iPS Cell Research and Application (CiRA), Kyoto University [11].

2.2. Methods

2.2.1. Generation of hiPSCs from the patient

CPT II deficiency-specific hiPSCs were derived from the patient by transducing the four reprogramming factors (OCT4, SOX2, KLF4, and c-MYC) or three factors (excluding c-MYC) into skin fibroblasts with retrovirus vectors as previously described [11,12]. In brief, fibroblasts derived from the CPT II-deficient patient were maintained and expanded in DMEM containing 10% fetal bovine serum. The patient fibroblasts were seeded in 6-well plates at 1.0×10^5 cells/well. The next day, the cells were infected with Slc7al lentiviruses with 4 μg/mL polybrene (Nacalai Tesque). Fibroblasts expressing the mouse Slc7al were seeded in 6-well plates at 1.0×10^5 cells/well 1 day before transduction. Equal amounts of four retrovirus-containing supernatants were mixed and supplemented with 4 μg/mL polybrene. Six days after transduction, the fibroblasts were replated onto mitomycin C-treated SNL feeder cells. Thirty days after transduction, iPSC colonies were selected for expansion.

2.2.2. Cell culture

CPT II-deficient hiPSCs were cultured as previously described [11]. The hiPSCs were grown on mitomycin C-treated SNL feeder cells in Primate ES medium (ReproCELL, Kanagawa, Japan) supplemented with 500 U/mL penicillin/streptomycin (Invitrogen, Carlsbad, CA) and 4 ng/mL recombinant human basic fibroblast growth factor (bFGF, Wako, Osaka, Japan). For routine passaging, hiPSC colonies were dissociated by an enzymatic method with CTK dissociation solution consisting of 0.25% trypsin (Invitrogen), 0.1% collagenase IV (Invitrogen), 20% knockout serum replacement (KSR, Invitrogen), and 1 mM $CaCl_2$ in PBS (Nacalai Tesque) and split at a ratio between 1:3 and 1:6.

2.2.3. Embryoid body (EB) formation

For EB formation, a 10-cm plate containing hiPSCs was rinsed with PBS and treated with 1 mg/mL type IV collagenase (Invitrogen) in DMEM for 10 min at 37 °C. The collagenase was rinsed away with PBS and replaced with undifferentiation medium. The cells were then scraped off with a cell scraper (IWAKI, Tokyo, Japan), dissociated by pipetting, and distributed into a low attachment 6-well plate (Corning, Tokyo, Japan) containing knockout-DMEM (Invitrogen) supplemented with 20% KSR, 0.1 mM non-essential amino acids (Invitrogen), 2 mM glutamine (Invitrogen), 500 U/mL penicillin/streptomycin, and 0.55 mM 2-mercaptoethanol (Invitrogen). After 8 days as a floating culture, the EBs were transferred to gelatin-coated plates and cultured in the same medium for another 8 days.

2.2.4. Teratoma formation

The undifferentiated iPSCs were harvested using CTK dissociation solution, collected, and centrifuged, and the pellets were resuspended in DMEM/F12 (Invitrogen). A quarter of the iPSCs from a confluent 10-cm plate was injected into the testes of a non-obese diabetic/severe combined immunodeficient (NOD-SCID mouse, CLEA, Tokyo, Japan). Nine to 12 weeks after injection, the tumors were dissected and fixed with PBS containing 4% paraformaldehyde (PFA). Paraffin-embedded tissues were sectioned and stained with hematoxylin and eosin.

2.2.5. Mutational analysis of the CPT2 in patient-derived iPSCs

Overlapping PCR primers that targeted CPT2 exons were designed to cover the entire coding region (Table 1; GenBank accession No. M58581). The PCR protocol was as follows: 30 cycles of 1 min at 94 °C for denaturation, 1 min at 60 °C for annealing, and 1 min at 72 °C for extension, followed by 1 cycle of 10 min at 60 °C for completion. Each PCR product was sequenced on an automated DNA sequencer (ABI 3100 Genetic Analyzer; Applied Biosystems Hitachi, Tokyo, Japan) by using the BigDye Terminator v3.1 cycle-sequencing kit (Applied Biosystems, Foster City, CA) and the sequencing primers listed in Table 1.

2.2.6. Induction of hiPSCs into skeletal muscle cells

We used our previously reported method in which *MYOD1* overexpression in undifferentiated hiPSCs efficiently and reproducibly induces differentiation into mature skeletal muscle cells within 10 days [13]. Briefly, we transduced a self-contained Tet-inducible MYOD1 expressing *piggyBac* vector (Tet-MYOD1 vector) and transposase into CPT II-deficient iPSCs by lipofection. This system allows the indirect monitoring of induced *MYOD1* expression in response to doxycycline (Dox) by co-expression of a red fluorescent protein (mCherry). It was also reported that low glucose culture conditions purified the cardiomyocytes from mouse and human iPSC differentiation cultures by selecting only cardiomyocytes, based on the findings of the substantial biochemical differences in glucose and lactate metabolism between cardiomyocytes and undifferentiated iPSCs [14]. We used a similar strategy to increase the purity of generated myocytes and cultured the hiPSC-derived differentiated cells with low glucose media (1.0 g/L) for an additional day after 10 days of myocyte induction by *MYOD1* overexpression. The low-glucose medium was composed of MEM (Sigma, St. Louis, MO) containing 0.4% bovine serum albumin (Sigma), 0.4 mM L-carnitine (Sigma), 0.2 mM unlabeled palmitic acid (Nacalai Tesque), and 500 U/mL penicillin/streptomycin. For

Table 1
Oligonucleotide sequences, related to Fig. 1. Sequences of primers used in this study.

Gene	Forward primer: 5′ to 3′	Reverse primer: 5′ to 3′
hOCT4Tg	GCTCTCCCATGCATTCAAACTGA	CCCTTTTTCTGGAGACTAAATAAA
hSOX2 Tg	TTCACATGTCCCAGCACTACCAGA	GACATGGCCTGCCCGGTTATTATT
hKLF4 Tg	CCACCTCGCCTTACACATGAAGA	GACATGGCCTGCCCGGTTATTATT
hcMYC Tg	ATACATCCTGTCCGTCCAAGCAGA	GACATGGCCTGCCCGGTTATTATT
hOCT4 Total	CCCCAGGGCCCCATTTTGGTACC	ACCTCAGTTTGAATGCATGGGAGAGC
hSOX2 Total	TTCACATGTCCCAGCACTACCAGA	TCACATGTGTGAGAGGGGCAGTGTGC
hKLF4 Total	GATTACGCGGGCTGCGGCAAAACCTACACA	TTAAAAATGTCTCTTCATGTGTAAGGCGAG
hcMYC Total	ATACATCCTGTCCGTCCAAGCAGA	TCACGCACAAGAGTTCCGTAGCTGTTCAAG
CPT2 exon1	CGGCCTTGTGTTTAGACTCC	CTTCCAGATTAGGGGCTGTG
CPT2 exon2	GCCTTACACTGACCCTGCTT	AGGTTCTGGGTTCCTGGAGA
CPT2 exon3	TTCCAGGTTTTAGGGCTATG	GGAGGATGAGACGTTACTTC
CPT2 exon4	TAGGGACAGCATTAACATTT	TGGCCTTGTCATCAGTGAAG
CPT2 exon4	GTCCCAGTATTTTCGGCTTT	TGTGGGACAAGTGGACAAGG
CPT2 exon4	GAGTTTCCCCTGGCATACCT	GCCTCCTCTCTGAAACTGGA
CPT2 exon4	ACAGCTGCTAAGGAAAAGTT	CAAGACCCAAGGGCATGCTC
CPT2 exon5	CTGAGACGCTGGTTTTCCA	GGTAGCTTTTCATCTGCCCA

immunostaining analyses of hiPSC-derived myocytes, human myosin heavy chain (MHC) antibody (R&D Systems, Minneapolis, MN) was used according to the manufacturer's instructions. Samples were observed under an inverted type fluorescence phase-contrast microscope (BZ-9000E; Keyence, Osaka, Japan).

2.2.7. In vitro probe assay of AC profiles

hiPSC-derived myocytes were cultured in a 6-well plate for 96 h with 1 mL medium A composed of MEM, 0.4% bovine serum albumin, 0.4 mM L-carnitine, 0.2 mM unlabeled palmitic acid, and 1% penicillin/streptomycin without L-glutamine, or medium B composed of medium A supplemented with 0.4 mM bezafibrate (Sigma) [15]. Cultured cells were incubated with medium A or B at 38 °C for 96 h to determine the effects of heat stress on mitochondrial FAO.

2.2.8. Quantitative acylcarnitine analysis

Acylcarnitine in the culture supernatant was analyzed by MS/MS (API 3000; Applied Biosystems).

2.2.9. Heat stimulation

Differentiated myocytes on culture day 9 were subjected to heat stress at 38 °C on a hot plate.

2.2.10. Regulated PCR array for skeletal muscle-related genes

To analyze the expression of skeletal muscle-related genes, we performed a regulated PCR array. For first-strand cDNA synthesis, 1 μg total RNA was reverse-transcribed in a 20-μl reaction mix and the RT^2 First Strand Kit (RT^2 Profiler PCR Array, SuperArray Bioscience, Frederick, MD) according to the manufacturer's instructions. qRT-PCR was performed with a CFX96 (Bio-Rad, Hercules, CA) and universal cycling conditions (10 min at 95 °C, 15 s at 95 °C, and 1 min at 60 °C for 40 cycles). The fold change in gene expression was determined by the comparative cycle Ct (ΔΔCt) method. Statistical calculations were based on the web-based RT^2 Profiler PCR Array Data Analysis (SuperArray Bioscience).

2.2.11. Microarray analysis

aRNA preparation, fragmentation, hybridization, and scanning of the GeneChip Human Genome U133 Plus 2.0 Array (Affymetrix, Santa Clara, CA) were performed according to manufacturer's protocols. Labeled aRNA was prepared with the GeneChip 3′IVT Express Kit (Affymetrix). Briefly, cDNA was generated from total RNA (100 ng), using reverse transcriptase and a T7-oligo (dT) primer. After second-strand cDNA synthesis, the cDNA was converted to aRNA by an *in vitro* transcription reaction with biotin-labeled ribonucleotides and T7 RNA polymerase. After synthesis, the aRNA was purified to remove enzymes, salts, and unincorporated nucleotides. The concentration of cRNA was determined from the absorbance at 260 nm in a UV spectrophotometer. The aRNA was fragmented at 94 °C in fragmentation buffer (Affymetrix). The samples were hybridized to the GeneChip(R) Human Genome U133 Plus 2.0 Arrays at 45 °C for 16 h with rotation (60 rpm) in an oven. The arrays were automatically washed and stained with the GeneChip Hybridization, Wash and Stain Kit (Affymetrix). The Probe Array was scanned using a GeneChip Scanner 3000 7G (Affymetrix). Intensity data and the CHP files were generated by Affymetrix GeneChip Command Console Software and Affymetrix Expression Console Software.

3. Results

3.1. Generation of CPT II-deficient iPSCs (CPTIID-iPSCs) from patient fibroblasts

The skin fibroblasts were converted into iPSCs after transduction with four retroviral vectors encoding OCT4, SOX2, KLF4, and c-MYC, or with three vectors (excluding c-MYC). Quantitative reverse-transcription PCR was used to evaluate the CPTIID-iPSC clones with repression of the exogenously introduced genes analyzed as the ratio of transgene (Tg) expression to total (endogenous and transgene) expression (Table 1). Based on these analyses, the iPSC clone with the highest level of repression was selected for further experiments. This clone exhibited characteristic human embryonic stem cell (ESC) morphology (Fig. 1A), expressed pluripotency markers, including OCT4, NANOG, SOX2, SSEA4, TRA-1-60, TRA-1-81, and alkaline phosphatase (AP) activity (Fig. 1B), and had a normal karyotype (Fig. 1C). The pluripotent properties of CPTIID-iPSCs were also assessed using embryoid body (EB) and teratoma formation upon intratesticular injection of undifferentiated CPTIID-iPSCs into NOD-SCID mice (Fig. 2A and B). Genetic identity was confirmed by STR analyses of the patient fibroblasts and iPSCs (data not shown). Mutation analysis of the causative gene revealed that the patient had compound heterozygous mutations in the *CPT2* [10]. Genomic analysis showed that both CPTIID-iPSCs and their parental fibroblasts possessed mutant CPT2 alleles (Fig. 1D). Sequencing from the 5′ and 3′ ends showed a CT deletion in the TCT at codon 408 (1223delCT), resulting in a stop signal at codon 420, and a sense mutation of arginine to cysteine at codon 631 (1891C→T; R631C). These results suggest that disease-specific iPSCs can be generated from the skin fibroblasts of a CPT II-deficient patient.

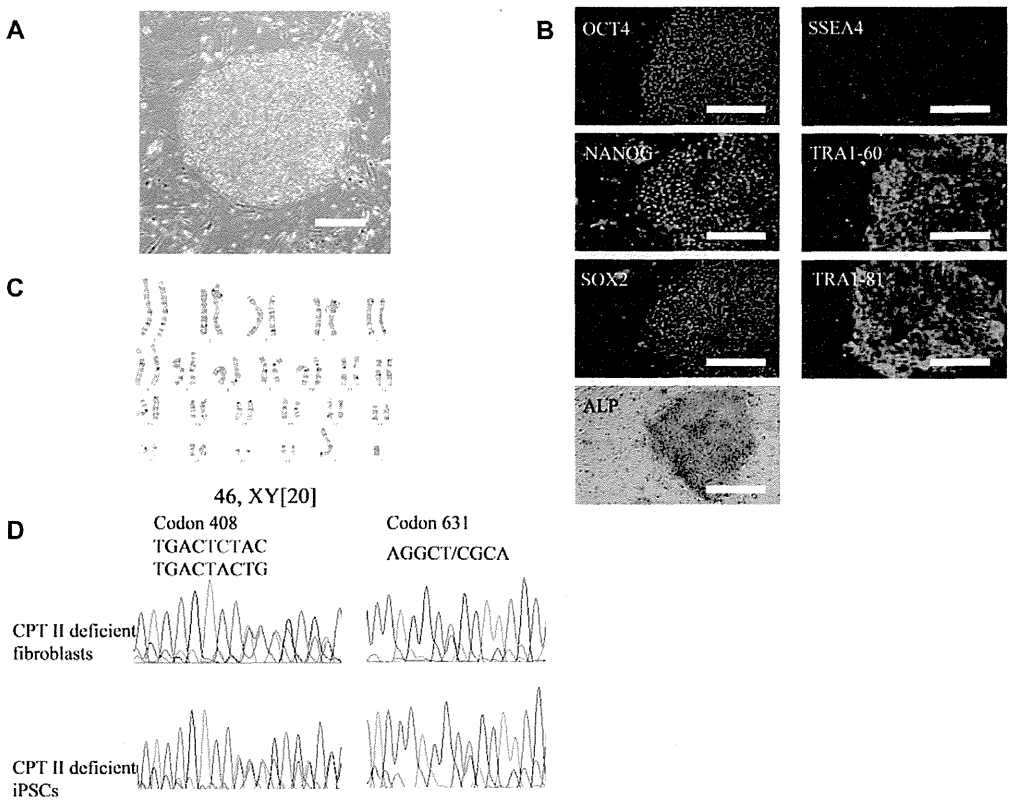

Fig. 1. Generation of iPSCs from a patient with CPT II deficiency. (A) Typical image of human embryonic stem cell (ESC)-like colony. Scale bars: 50 μm. (B) Immunocytochemistry for OCT4, NANOG, SOX2, SSEA4, TRA1-60 and TRA1-81, and the examination of alkaline phosphatase (AP) enzyme activity. Nuclei were stained with Hoechst 33342 (blue). Scale bars: 100 μm. (C) Karyotype analyses of CPT II-deficient iPSCs. (D) Mutational analyses of CPT II-deficient iPSCs and their parental fibroblasts. Sequencing from the 5′ and 3′ ends reveals a CT deletion from the TCT at codon 408, and an arginine to cysteine substitution at codon 631.

3.2. Differentiation of CPTIID-iPSCs into mature myocytes

We next examined whether the patient-derived iPSCs could be differentiated into myocytes, the target cell type of CPT II deficiency. We recently reported a highly efficient myocyte differentiation method based on overexpression of the *MYOD1* gene, a master regulator of myocyte lineage differentiation, in undifferentiated hiPSCs [13]. Tohyama et al. reported a non-genetic method for purifying cardiomyocytes in mouse and human iPSC differentiation cultures [14]. Their strategy is based on the substantial biochemical differences in glucose and lactate metabolism between cardiomyocytes and non-cardiomyocytes, including undifferentiated iPSCs. We used a combination of these strategies to generate myocytes from CPTIID-iPSCs. We transduced a Tet-MYOD1 vector and transposase into CPTIID-iPSCs by lipofection. We forced expression of *MYOD1* with Dox in undifferentiated CPTIID-iPSCs for 10 days. We then used low glucose medium for an additional day to select myocytes. After culture in low glucose medium, the remaining undifferentiated cells disappeared, and the differentiated cells survived, yielding myocyte generation at 50%–60% induction efficiency.

We confirmed the presence of mature myocytes by staining with anti-human MHC antibody (Fig. 3A). Electron microscopy revealed that differentiated myocytes derived from CPTIID-iPSCs had myofibrils containing mature myosin fibers and Z line-like structures (Fig. 3B). We also performed a PCR array and unsupervised clustering to generate myogenic gene profiles for myocytes differentiated from CPTIID-iPSCs, myocytes from control iPSCs (201B7), undifferentiated CPTIID-iPSCs, and undifferentiated 201B7 cells (Fig. 3C, Table 2). We confirmed the upregulation of markers of skeletal muscle contractility, skeletal myogenesis, and skeletal muscle autocrine signaling in myocytes differentiated from CPTIID-iPSCs compared to undifferentiated CPTIID-iPSCs. The expression patterns of muscle-related genes also differed between myocytes derived from CPTIID-iPSCs and control myocytes. These results suggest that mature myocytes can be efficiently generated from CPTIID-iPSCs by introducing a master transcriptional regulator of myocyte differentiation, MYOD1, and culturing in low glucose conditions.

3.3. Acylcarnitine (AC) profiles of the CPT II-deficient myocytes

An acylcarnitine profile determined by tandem mass spectrometry is essential for the definitive diagnosis of CPT II deficiency [15]. We thus examined the profile in myocytes differentiated from CPTIID-iPSCs. CPT II-deficient myocytes accumulated more C16 (palmitoylcarnitine) than did control myocytes (Fig. 4). Results were similar in myocytes differentiated from other iPSC clones from the same patient in this study (data not shown). These data indicated that patient-derived iPSCs recapitulated one of the clinical features of CPT II deficiency.

We previously reported that fibroblasts from patients with LCFA β-oxidation disorders, including CPT II deficiency, were more susceptible to heat stress in comparison to the fibroblasts of patients with medium-chain fatty acid β-oxidation disorders or healthy controls [15]. We thus investigated the effects of heat stress on myocytes derived from CPTIID-iPSCs and found that this treatment significantly increased C16 in CPT II-deficient cells, but not in controls (Fig. 4). We also demonstrated that bezafibrate, an agonist of peroxisome proliferator-activated receptor (PPAR), restores FAO activity in fibroblasts

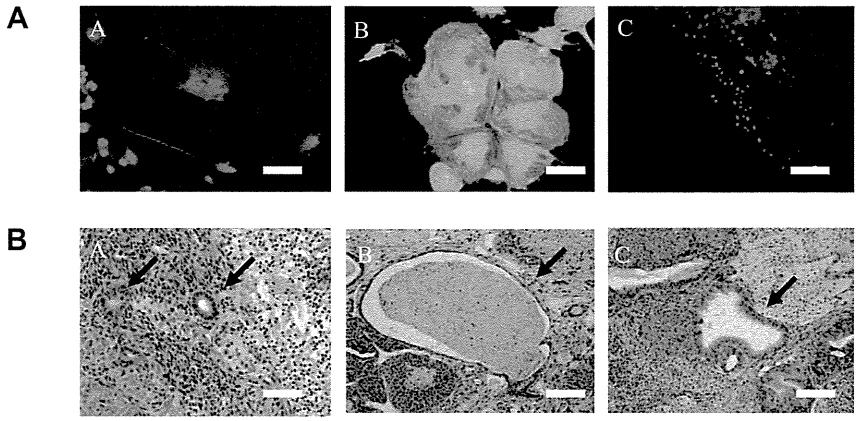

Fig. 2. Embryoid body (EB)- and teratoma-mediated differentiation of CPT II-deficient iPSCs. (A) Immunostaining of EBs generated from CPT II-deficient iPSCs for TUJ1 (ectoderm, A), α-SMA (mesoderm, B), and SOX17 (endoderm, C). Nuclei were stained with Hoechst 33342 (blue). Scale bars: 100 μm. (B) Hematoxylin and eosin staining of histological sections of teratomas derived from CPT II-deficient iPSCs. Neural tissues (ectoderm, A), cartilage (mesoderm, B), gut-like epithelia (endoderm, C). Scale bars: 100 μm.

with CPT II deficiency [15]. We investigated the effects of bezafibrate on myocytes derived from CPTIID-iPSCs. At 37 °C and 38 °C, bezafibrate decreased C16 levels in controls and CPT II-deficient myocytes. In the CPT II-deficient myocytes, bezafibrate at 37 °C reduced C16 levels to those observed in controls (Fig. 4). These results suggest that mature myocytes derived from CPTIID-iPSCs recapitulate some of the phenotypes associated with CPT II deficiency.

4. Discussion

Rhabdomyolysis occurs after exhaustive exercise or severe infection without trauma or drugs in CPT II deficiency. The adult-onset form presents with myoglobinuria and myalgia, frequently leading to acute renal failure. Rhabdomyolysis may repeatedly develop within the same families. Hereditary rhabdomyolysis is often caused by compromised enzymatic activity associated with LCFA metabolism.

Accurate experimental modeling of the disease and its response to clinical intervention are hampered due to a lack of appropriate animal models. To address this issue, we sought to derive iPSCs from a patient with CPT II deficiency, who had a history of repetitive rhabdomyolysis and acute renal failure. There have been no reports of derivation of iPSCs from patients with FAO disorders, including CPT II deficiency, and to the best of our knowledge, we are the first to report the successful generation of iPSCs from a CPT II-deficient patient.

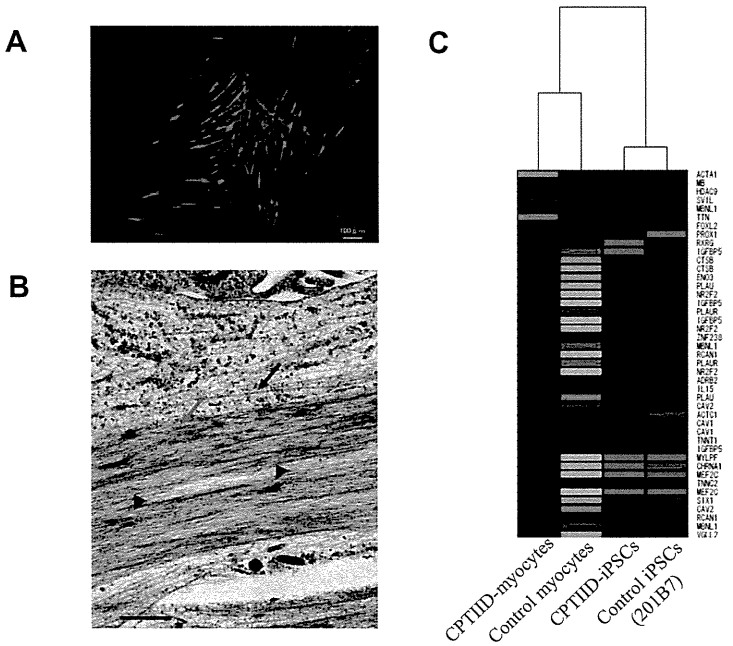

Fig. 3. Directed differentiation of CPT II-deficient iPSCs into skeletal muscle cells. (A) Immunocytochemistry of the myocytes derived from CPT II-deficient iPSCs with anti-human Myosin Heavy Chain (MHC) antibody. Nuclei were stained with Hoechst 33342 (blue). Scale bar: 100 μm. (B) Structural analysis of myocytes differentiated from CPT II-deficient iPSCs by electron microscopy. A red arrow indicates myofibrils. Black arrowheads indicate immature Z lines. A black arrow indicates myosin fibers. Scale bar: 500 nm. (C) Characterization of iPSC-derived myocytes. Myogenic gene profiles and unsupervised clustering based on markers associated with myocytes in undifferentiated iPSCs and differentiated myocytes. CPTIID-myocytes, control myocytes, CPTIID-iPSCs, and control iPSCs. Green indicates up-regulated genes and red indicates down-regulated genes. Up-regulated genes were identified by changes of at least 2-fold. CPTIID-myocytes; Myocytes differentiated from CPTIID-iPSCs.

Table 2
The expression of markers for skeletal muscle contractility, skeletal myogenesis, and skeletal muscle autocrine signaling in the myocytes differentiated from CPT II-deficient iPSCs. Gene expression was evaluated using quantitative real time RT-PCR as described in Materials and Methods; GAPDH was the internal control. Results are shown as fold change relative to control samples of undifferentiated CPT II-deficient iPSCs.

	Symbol	Fold change
Skeletal muscle contractility	ATP2A1	4.6
	CAV3	22.0
	DES	33.5
	DMPK	2.1
	DYSF	2.2
	LMNA	3.9
	MB	8.3
	MYH1	86.5
	MYOT	4.0
	NEB	4.3
	SGCA	4.1
	TNNC1	4.1
	TNNI2	8.4
	TNNT1	2.2
	TNNT3	35.7
	TTN	6.4
Skeletal myogenesis	ACTA1	7.4
	CAPN2	3.1
	CAV1	3.8
	IGF1	5.7
	IGFBP3	5.9
	IGFBP5	15.1
	MEF2C	43.3
	MSTN	74.8
	MUSK	11.0
	MYOG	477.3
	PAX3	2.7
Skeletal muscle autocrine signaling	IGF1	5.7
	IGF2	59.7
	IL6	3.2

Many somatic cell types have been generated from iPSCs, but there have been limited reports describing directed differentiation into myocyte lineages [13]. Our protocol was used to generate CPT II-deficient myocytes from CPTIID-iPSCs [13]. These processes were validated by the detection of genes involved in skeletal muscle development and function in CPT II-deficient myocytes. Culture in low glucose caused the death of undifferentiated iPSCs, which require large quantities of glucose, while the differentiated cells require limited glucose and produce lactic and pyruvic acids to more effectively obtain energy by mitochondrial oxidative phosphorylation. Thus, by using low-glucose medium, we increased the differentiation efficiency of iPSC-derived myocytes.

Yamaguchi et al. showed that an *in vitro* AC profiling assay could reliably detect various FAO disorders, consistent with reports from other groups [16–18]. In particular, C16 accumulation was found to be a reliable biomarker that could be used to diagnose CPT II deficiency. Consistent with these findings, our hiPSC-derived myocytes mimicked the metabolic characteristics of the disease.

The effects of PPAR agonists on mitochondrial FAO have been extensively examined [19]. Bezafibrate has proven efficacy in the treatment of long-chain FAO disorder [20–24]. We found that bezafibrate reduced long-chain ACs more effectively in myocytes from patient-derived iPSCs than in those from control hiPSCs. These findings indicate that bezafibrate could be a therapeutic drug for CPT II deficiency and other mitochondrial FAO disorders.

In conclusion, we successfully derived disease-specific iPSCs from a patient with CPT II deficiency and differentiated them into myocytes. Our results suggest that cellular models using patient-derived iPSCs will be of significant benefit for research groups studying CPT II deficiency-related diseases, and that these iPSC disease models may be a valuable resource for testing novel therapeutic strategies for these disorders.

Conflict of interest

The authors declare that they have no conflict of interest.

Acknowledgments

We thank Ms. Y Sasaguri for technical and secretarial assistance and Dr. S Mae for technical support and helpful discussion. This work was supported in part by research funds no. 101001 (H.K.) and no. 122502 (T.Y.) from the Central Research Institute of Fukuoka University, a Grant-in-Aid for Scientific Research from the Japan Society for Promotion of Science (23791200, 25870995

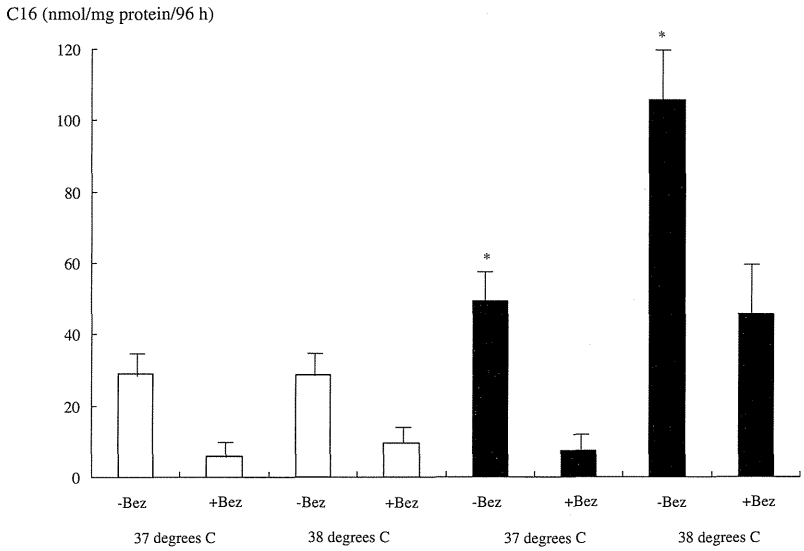

Fig. 4. Acylcarnitine (AC) profiles in culture medium of iPSC-derived myocytes loaded with palmitic acid after bezafibrate (Bez) treatment. Data are shown as mean ± SD (nmol/mg protein/96 h) ($n = 3$) White bars: Myocytes from control iPSCs; Black bars: Myocytes from CPT II-deficient iPSCs. Statistically significant differences between 37 °C Bez (-) of control and 37 °C or 38 °C Bez (-) of patients shown as $^*p < 0.05$.

to T.Y.), Takahashi Industrial and Economic Research Foundation, and Kaibara Morikazu Medical Science Promotion Foundation. This work was also supported by the Japan Society for the Promotion of Science (JSPS) through its "Funding Program for World-Leading Innovative R&D on Science and Technology (FIRST Program)" to K.O. and by the Japan Science and Technology Agency (JST) through its research grant "Core Center for iPS Cell Research, Research Center Network for Realization of Regenerative Medicine" to K.O.

References

[1] H.C. Faigel, Carnitine palmitoyltransferase deficiency in a college athlete: a case report and literature review, J. Am. Coll. Health 44 (1995) 51–54.
[2] K.J. Kelly, J.S. Garland, T.T. Tang, A.L. Shug, M.J. Chusid, Fatal rhabdomyolysis following influenza infection in a girl with familial carnitine palmitoyl transferase deficiency, Pediatric 84 (1989) 312–316.
[3] J.P. Keverline, Recurrent rhabdomyolysis associated with influenza-like illness in a weight-lifter, J. Sports Med. Phys. Fitness 38 (1998) 177–179.
[4] J.P. Bonnefont, F. Demaugre, C. Prip-Buus, J.M. Saudubray, M. Brivet, et al., Carnitine palmitoyltransferase deficiencies, Mol. Genet. Metab. 68 (1999) 424–440.
[5] P.J. Isackson, M.J. Bennett, G.D. Vladutiu, Identification of 16 new disease-causing mutations in the *CPT2* gene resulting in carnitine palmitoyltransferase II deficiency, Mol. Genet. Metab. 89 (2006) 323–331.
[6] N.S. Ross, C.L. Hoppel, Partial muscle carnitine palmitoyltransferase-A deficiency. Rhabdomyolysis associated with transiently decreased muscle carnitine content after ibuprofen therapy, JAMA 257 (1987) 62–65.
[7] P.L. Blanc, H. Carrier, L. Thomas, J.M. Chavaillon, D. Robert, Acute rhabdomyolysis with carnitine-palmitoyl-transferase deficiency, Intensive Care Med. 8 (1982) 307.
[8] M. Kottlors, M. Jaksch, U.P. Ketelsen, S. Weiner, F.X. Glocker, et al., Valproic acid triggers acute rhabdomyolysis in a patient with carnitine palmitoyltransferase type II deficiency, Neuromuscul. Disord. 11 (2001) 757–759.
[9] H. Katsuya, M. Misumi, Y. Ohtani, T. Miike, Postanesthetic acute renal failure due to carnitine palmitoyl transferase deficiency, Anesthesiology 68 (1998) 945–948.
[10] H. Kaneoka, N. Uesugi, A. Moriguchi, S. Hirose, M. Takayanagi, et al., Carnitine palmitoyltransferase II deficiency due to novel gene variant in a patient with rhabdomyolysis and ARF, Am. J. Kidney Dis. 45 (2005) 596–602.
[11] K. Takahashi, K. Tanabe, M. Ohnuki, M. Narita, T. Ichisaka, et al., Induction of pluripotent stem cells from adult human fibroblasts by defined factors, Cell 131 (2007) 861–872.
[12] J. Yu, M.A. Vodyanik, K. Smuga-Otto, J. Antosiewicz-Bourget, J.L. Frane, et al., Induced pluripotent stem cell lines derived from somatic cells, Science 318 (5858) (2007) 1917–1920.
[13] A. Tanaka, K. Woltjen, K. Miyake, A. Hotta, M. Ikeya, et al., Efficient and reproducible myogenic differentiation from human iPS cells, PLoS One 8 (2013) e61540.
[14] S. Tohyama, F. Hattori, M. Sano, T. Hishiki, Y. Nagahata, et al., Distinct metabolic flow enables large-scales purification of mouse and human pluripotent stem cell-derived cardiomyocytes, Cell Stem Cell 12 (2013) 127–137.
[15] H. Li, S. Fukuda, Y. Hasegawa, H. Kobayashi, J. Purevsuren, et al., Effect of heat stress and bezafibrate on mitochondrial β-oxidation: comparison between cultured cells from normal and mitochondrial fatty acid oxidation disorder children using *in vitro* probe acylcarnitine profiling assay, Brain Dev. 32 (2010) 362–370.
[16] S. Yamaguchi, Newborn screening in Japan: restructuring for the new era, Ann. Acad. Med. Singapore 37 (2008) 13–15.
[17] J.G. Okun, S. Kolker, A. Schulze, D. Kohlmuller, K. Olgemoller, et al., A method for quantitative acylcarnitine profiling in human skin fibroblasts using unlabelled palmitic acid: diagnosis of fatty acid oxidation disorders and differentiation between biochemical phenotypes of MCAD deficiency, Biochim. Biophys. Acta 1584 (2002) 91–98.
[18] K.G. Sim, K. Carpenter, J. Hammond, J. Christodoulou, B. Wilcken, Acylcarnitine profiles in fibroblasts from patients with respiratory chain defects can resemble those from patients with mitochondrial fatty acid beta-oxidation disorders, Metabolism 51 (2002) 366–371.
[19] G.D. Barish, V.A. Narkar, R.M. Evans, PPAR delta: a dagger in the heart of the metabolic syndrome, J. Clin. Invest. 116 (2006) 590–597.
[20] F. Djouadi, J. Bastin, PPARs as therapeutic targets for correction of inborn mitochondrial fatty acid disorders, J. Inherit. Metab. Dis. 31 (2008) 217–225.
[21] S. Gobin-Limballe, F. Djouadi, F. Aubey, S. Olpin, B.S. Andresen, et al., Genetic basis for correction of very-long-chain acyl-coenzyme A dehydrogenase deficiency by bezafibrate in patient fibroblasts: toward a genotype-based therapy, Am. J. Hum. Genet. 81 (2007) 1133–1143.
[22] F. Djouadi, F. Aubey, D. Schlemmer, S. Gobin, P. Laforet, et al., Potential of fibrates in treatment of fatty acid oxidation disorders: revival of classical drugs?, J Inherit. Metab. Dis. 29 (2006) 341–342.
[23] F. Djouadi, J.P. Bonnefont, L. Thuillier, V. Droin, N. Khadom, et al., Correction of fatty acid oxidation in carnitine palmitoyl transferase 2-deficient cultured skin fibroblasts by bezafibrate, Pediatr. Res. 54 (2003) 446–451.
[24] F. Djouadi, F. Aubey, D. Schlemmer, J.P. Ruiter, R.J. Wanders, et al., Bezafibrate increases very-long-chain acyl-CoA dehydrogenase protein and mRNA expression in deficient fibroblasts and is a potential therapy for fatty acid oxidation disorders, Hum. Mol. Genet. 14 (2005) 2695–2703.

Sapropterin Is Safe and Effective in Patients less than 4-Years-Old with BH_4-Responsive Phenylalanine Hydroxylase Deficiency

Haruo Shintaku, MD, PhD[1], and Toshihiro Ohura, MD, PhD[2]

Objective To assess the safety and efficacy of tetrahydrobiopterin therapy with sapropterin to treat tetrahydrobiopterin (BH_4)-responsive phenylalanine hydroxylase (PAH) deficiency in children aged <4 years compared with those aged ≥4 years.

Study design We analyzed a longitudinal follow-up study conducted in all patients with BH_4-responsive PAH deficiency throughout Japan. At the end of 2011, 43 patients were receiving sapropterin, of whom 21 were aged <4 years at the initiation of treatment. The starting dose of sapropterin was ≥10 mg/kg/day in 11 of these 21 patients. The duration of follow-up was ≥4 years in 6 of those 11 patients; 3 of these 6 were followed for ≥10 years. Nine patients were receiving sapropterin monotherapy at the end of 2011.

Results Serum phenylalanine level was maintained within the recommended optimal control range in all 21 patients who started sapropterin treatment before age 4 years. Only 1 nonserious adverse drug reaction occurred, an elevated alanine aminotransferase level in 1 patient. No significant abnormal behavior related to nerve disorders was reported.

Conclusion Sapropterin therapy initiated before age 4 years was effective in maintaining serum phenylalanine level within the favorable range and was safe in Japanese patients with BH_4-responsive PAH deficiency. *(J Pediatr 2014;165:1241-4).*

Based on clinical trial data, sapropterin dihydrochloride, a tetrahydrobiopterin (BH_4) drug, has been approved for the treatment of BH_4-responsive phenylalanine hydroxylase (PAH) deficiency in patients aged ≥4 years in the US. Since the drug's approval, however, many patients aged <4 years have been treated with sapropterin. In Japan, sapropterin dihydrochloride granules 2.5% (Biopten, Daiichi Sankyo, Japan) was approved in 1992 for treatment of BH_4 deficiency and in 2008 for treatment of BH_4-responsive PAH deficiency.

We previously reported the safety and efficacy of long-term (16 years) treatment with sapropterin in BH_4-deficient patients who started treatment before age 4 years based on postmarketing surveillance in Japan.[1] Here we report on the long-term safety and efficacy of sapropterin in patients with BH_4-responsive PAH deficiency who started treatment before age 4 years.

Methods

At the end of 2011, 43 patients in Japan were receiving BH_4 therapy with sapropterin, 21 of whom were aged <4 years at the start of treatment. Only 1 patient aged ≥4 years was hospitalized. One child aged <4 years and 6 children aged ≥4 years had a BH_4-responsive sibling. All patients had undergone neonatal phenylketonuria screening and pteridine analysis, along with a dihydropteridine reductase assay that identified them as not BH_4-deficient.[2]

The present postmarketing surveillance study was conducted in 21 medical centers in Japan between 1995 and 2011. During this period, serum phenylalanine (Phe) concentrations were measured using an automated amino acid analyzer (L-8800; Hitachi, Tokyo, Japan), and serum pteridine concentrations were measured by high-performance liquid chromatography (LC-10; Shimazu, Kyoto, Japan) after iodine oxidation. Dihydropteridine reductase activity was measured using Guthrie card specimens, as described previously.[2]

A 1-week loading test (20 mg/kg/day in 2 doses for 7 consecutive days) was performed to evaluate BH_4 responsiveness. A 30% decrease in Phe level was defined as BH_4-responsive hyperphenylalaninemia.

Results

The clinical characteristics of the study patients and serum Phe levels before sapropterin treatment are presented in Table I. The study cohort comprised 21

BH_4	Tetrahydrobiopterin
PAH	Phenylalanine hydroxylase
Phe	Phenylalanine

From the [1]Department of Pediatrics, Osaka City University School of Medicine, Osaka, Japan; and [2]Department of Pediatrics, Tohoku University School of Medicine, Sendai, Japan

Supported by the Ministry of Health, Labour and Welfare, Japan (grant 14427732 to H.S. to produce the manuscript). H.S. received the data of postmarketing surveillance of Biopten for BH_4-responsive hyperphenylalaninemia. H.S. and T.O. received consultant, travel, and lecture fees from Daiichi Sankyo. The authors declare no conflict of interest.

Portions of the study were presented as a poster at International Congress of Inborn Errors of Metabolism, Barcelona, Spain, September 4, 2013.

http://dx.doi.org/10.1016/j.jpeds.2014.08.003

Table I. Patient characteristics, serum Phe level before BH_4 treatment, and BH_4 duration and dose

Characteristics	Age at administration <4.0 y	Age at administration ≥4.0 y
Sex, n		
Male	10	12
Female	11	10
Age as of December 2011, y, n		
<1	1	0
1 to <4	9	0
4 to <10	8	9
10 to <16	2	12
>16	1	1
Age at administration, y, n		
<1	8	0
1 to <4	13	0
4 to <10	0	18
10 to <16	0	3
>16	0	1
Complications, n		
No	17	15
Yes	4	7
BH_4 combined with diet therapy (at the end of 2011)		
No	9	10
Yes	12	12
Treatment duration, y, n		
<1	2	3
1-3	13	18
4-6	1	0
7-10	2	0
>10	3	1
BH_4 dose, mg/kg, n		
<5	2 (3)*	2 (3)*
5 to <10	8 (7)*	11 (11)*
10 to <15	8 (7)*	5 (6)*
15 to <20	1 (3)*	3 (1)*
≥20	2 (1)*	1 (1)*
Serum Phe level before BH_4 treatment, μmol/L, mean ± SD (range)		
Mass screening (at 5 d after birth)	472.1 ± 149.5 (224.2-818.1)	667.8 ± 282.4 (242.4-1187.3)
First visit (at hospital visit for thorough checkup)	479.3 ± 214.0 (169.7-981.8)	673.0 ± 521.5 (66.7-2230.3)
Initial investigation (before BH_4-loading test)	280.0 ± 146.8 (78.8-757.6)	420.7 ± 272.0 (161.2-1266.7)

*Number of patients at initiation (at the end of 2011).

patients in whom treatment was initiated at age <4 years. The duration of treatment was ≥4 years in 6 of the 21 patients, ≥10 years in 3 of those 6 patients, and >16 years in 1 of the latter 3 patients.

Serum Phe levels were reduced in response to 3 different BH_4-loading tests. The average reduction in serum Phe level was 42.2% in the single-loading test, 42.0% in the 4-times loading test, and 55.4% in the 1-week loading test, with respective cutoff values of 20%, 30%, and 50%.[3] Based on these data, all 21 patients were diagnosed with BH_4-responsive PAH deficiency (Figure 1).

Phe level according to age at the end of 2011 are shown in Figure 2, in all patients and by age at treatment initiation (<4 years or ≥4 years). In 11 of the 21 patients who started sapropterin therapy before age 4 years, the initial dose was >10 mg/kg day (Table I). The duration of follow-up was >4 years in 6 of these 11 patients, and >10 years in 3 of the latter 6 patients (Table I). At the end of the study period, 9 of the 21 patients were receiving sapropterin monotherapy.

After 4 years of age all patients were treated with sapropterin. Serum Phe levels were maintained within a favorable range in both groups, with no significant difference between the groups (Figure 2). Serum Phe levels were maintained within a favorable range in the 21 patients who started treatment before age 4 years, but were variable (ranging from too low to too high) in the 22 patients who did so after age 4 years (Figure 2). However, there was no significant difference in mean Phe concentration before BH_4 therapy between the 2 age groups.

All patients responded to sapropterin treatment, showing reductions in serum Phe levels to within the recommended optimal control range. Among the 43 patients, 19 were treated with only sapropterin and 24 were treated with sapropterin plus diet therapy. The mean serum Phe levels was 368.4 μmol/L in the patients who received sapropterin monotherapy and 362.4 μmol/L in those who received sapropterin with diet therapy, a statistically nonsignificant difference ($P = .10$).

Examination of electroencephalograms performed in 7 patients revealed no abnormalities, and brain magnetic resonance imaging showed an abnormality in only 1 of 8 patients. Adverse events are reported in Table II. Only 1 nonserious adverse drug reaction occurred, a mild increase in alanine aminotransferase level that improved without the need to stop sapropterin therapy. All 21 patients have since developed normally, and all of those who have reached school age are now attending normal schools.

Discussion

Patients with BH_4-responsive PAH deficiency, many of whom carry the *R241C* allele, respond to BH_4 administration. Although no clear correlation was seen between the reduced serum Phe levels in the BH_4-loading tests and *PAH* gene mutations, at least 1 mild phenylketonuria mutation or missense mutation was found in patients with BH_4-responsive PAH deficiency.[3]

Notably, the duration of treatment was ≥4 years in 6 of the 21 patients, ≥10 years in 3 of those 6 patients, and >16 years in 1 of these latter 3 patients (who was treated for hyperphenylalaninemia without BH_4 deficiency). This study represents a unique long-term follow-up of patients with BH_4-responsive PAH deficiency. BH_4-responsive PAH deficiency was first reported by Kure et al[4] in 1999. All 43 patients with BH_4-responsive PAH deficiency in Japan have been treated with BH_4 therapy. Sapropterin was approved for treating BH_4 deficiency in 1992 in Japan.

Our findings show that the control of serum Phe level in patients with BH_4-responsive PAH deficiency is more even and effective when sapropterin treatment is initiated before age 4 years (Figure 2), although there was no significant difference in mean Phe level between the 2 age groups. In the patients who started treatment at age ≥4 years,

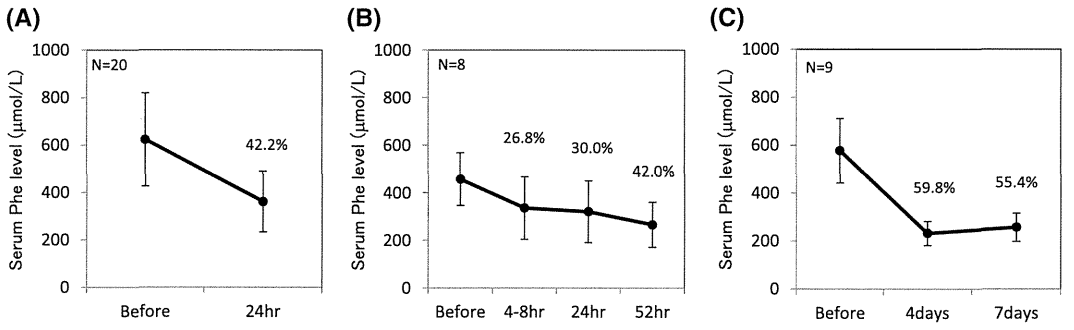

Figure 1. Serum Phe levels and response to BH_4-loading tests. **A,** Single loading test (cutoff, 20%). **B,** Four-times loading test (cutoff, 30%). **C,** One-week administration test (cutoff, 50%).

Phe levels varied more outside of the optimal range (Figure 2). Furthermore, during their first 4 years of life, it appears that Phe levels were better controlled within the optimal range by sapropterin therapy than by diet therapy, which can lower Phe levels to an excessive degree (Figure 2). At the end of this study, 19 of the 43 patients with BH_4-responsive PAH deficiency were treated with sapropterin monotherapy (Table I), and there was no significant difference in Phe level between the group treated with sapropterin monotherapy and the group treated with sapropterin plus diet therapy.

Sapropterin therapy is safe in this patient population, which is reassuring because treatment of BH_4-responsive PAH deficiency requires lifetime administration. Of the 21 patients who started treatment before age 4 years, 8 were aged <1 year, and treatment proved safe and effective in these children. No adverse side effects were reported, and there was no drug-related discontinuation of treatment.

Our safety results are supported by recent reports of sapropterin therapy in 147 patients with BH_4-responsive PAH deficiency with up to 12 years of follow-up in Europe that showed no severe adverse events; only 3 patients experienced adverse events, all of which disappeared when the dose was lowered.[5] Leuret et al[6] evaluated 15 patients under age 4 years who received sapropterin therapy and concluded, in agreement with our findings, that BH_4 therapy is efficient and safe before age 4 years in patients with BH_4-responsive PAH deficiency.

In the US, sapropterin was approved in 2007, and thus there is only 6 years of safety data on the use of this drug. In addition, the clinical trials for drug approval were conducted in children aged ≥4 years. Thus, the results of our study, with the longest follow-up reported to date, provide important assurance that long-term treatment with sapropterin is safe and effective in patients with BH_4-responsive PAH deficiency. ■

Submitted for publication Apr 5, 2014; last revision received Jul 8, 2014; accepted Aug 5, 2014.

Reprint requests: Haruo Shintaku, MD, PhD, Department of Pediatrics, Osaka City University Graduate School of Medicine, 1-4-3 Asahimachi, Abeno-ku, Osaka 545-8585, Japan. E-mail: shintakuh@med.osaka-cu.ac.jp

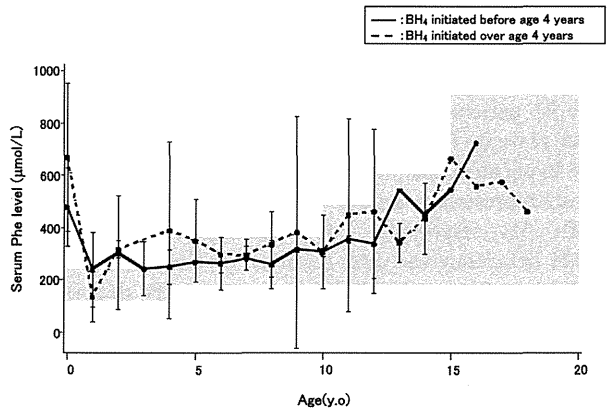

Figure 2. Phe levels according to patient age at treatment initiation and at the end of the study period. The *shaded area* indicates the recommended optimal control range.

Table II. Adverse events

Adverse events	Age at administration <4 y	Age at administration ≥4 y
All adverse events, n (%)	7 (33.3)	7 (31.8)
Infection and infestation, n (%)	5 (23.8)	4 (18.2)
Impetigo	0 (0.0)	1 (4.6)
Influenza	1 (4.8)	1 (4.6)
Nasopharyngitis	2 (9.5)	2 (9.1)
Adenoiditis	1 (4.8)	0 (0.0)
Varicella	1 (4.8)	1 (4.6)
Respiratory, thoracic, and mediastinal disorders, n (%)	3 (14.3)	3 (13.6)
Allergic rhinitis	0 (0.0)	2 (9.1)
Upper respiratory inflammation	3 (14.3)	2 (9.1)
Clinical blood test, n (%)	1 (4.8)	0 (0.0)
Alanine aminotransferase elevation*	1 (4.8)	0 (0.0)
Injury, poisoning, and procedural complications, n (%)	1 (4.8)	1 (4.6)
Clavicle fracture	0 (0.0)	1 (4.6)
Skin laceration	1 (4.8)	0 (0.0)

Multiple events occurred in 1 patient.
*Side effect (nonserious).

References

1. Shintaku H, Ohwada M. Long-term follow-up of tetrahydrobiopterin therapy in patients with tetrahydrobiopterin deficiency in Japan. Brain Dev 2013;35:406-10.
2. Shintaku H. Disorders of tetrahydrobiopterin metabolism and their treatment. Curr Drug Metab 2002;3:123-31.
3. Shintaku H, Kure S, Ohura T, Okano Y, Ohwada M, Sugiyama N, et al. Long-term treatment and diagnosis of tetrahydrobiopterinresponsive hyperphenylalaninemia with a mutant phenylalanine hydroxylase gene. Pediatr Res 2004;55:425-30.
4. Kure S, Hou DC, Ohura T, Iwamoto H, Suzuki S, Sugiyama N, et al. Tetrahydrobiopterin-responsive phenylalanine hydroxylase deficiency. J Pediatr 1999;135:375-8.
5. Keil S, Anjema K, van Spronsen FJ, Lambruschini N, Burlina A, Bélanger-Quintana A, et al. Long-term follow-up and outcome of phenylketonuria patients on sapropterin: a retrospective study. Pediatrics 2013;131:e1881-8.
6. Leuret O, Barth M, Kuster A, Eyer D, de Parscau L, Odent S, et al. Efficacy and safety of BH_4 before the age of 4 years in patients with mild phenylketonuria. J Inherit Metab Dis 2012;35:975-81.

50 Years Ago in *THE JOURNAL OF PEDIATRICS*

Familial Extrahepatic Biliary Atresia?

Krauss AN. J Pediatr 1964;65:933-7

In 1964, Krauss reported cholestasis in a pair of siblings. His diagnosis of "extrahepatic familial biliary atresia" can be referenced to highlight the growing understanding of the spectrum of neonatal cholestasis that has occurred over the past 50 years.

The "differential" diagnosis for neonatal cholestasis in the 1960s was fairly simple, consisting of 3 main categories: (1) biliary atresia, which constituted roughly 25% of cases; (2) viral induced injury—toxoplasmosis, other, rubella, cytomegalovirus, and herpes simplex virus (TORCH)—infections, which were identified in less than 10%; and (3) "neonatal hepatitis," a misleading term referring to infants whose histologic findings included giant cell transformation of unknown etiology that served as a wastebasket diagnosis for roughly 65% of the infants who presented with elevated liver enzymes and jaundice. "Neonatal hepatitis" was idiopathic and often classified as sporadic or familial depending on the history.

Today, the landscape of neonatal cholestasis is much more defined. Alpha-1 antitrypsin deficiency, metabolic diseases, progressive familial intrahepatic cholestasis, bile acid synthetic defects, and Alagille syndrome are only a few of the now well-described processes that have reduced the percentage of infants with idiopathic neonatal cholestasis to about 10% of cases. This exponential expansion of knowledge that has culminated in the current understanding of the biologic basis of neonatal cholestatic syndromes paralleled the growth and development of the new subspecialty of pediatric hepatology.[1]

Although the precise etiology of biliary atresia remains unknown, it has not been documented to reoccur in a family member subsequently. Therefore, re-visiting Krauss' report today, one cannot help but consider an alternative diagnosis. A leading candidate would be Alagille syndrome given the cardiac and renal abnormalities identified in the publication. Unfortunately for the brothers in Krauss' report, Daniel Allagille's seminal article describing the autosomal dominant, multisystem disorder that now carries his name would not be published for another 5 years.[2]

Despite the advances, looking forward to the next 50 years it is clear that there is work to be done. As noted, up to 10% of infants presenting today with jaundice and elevated liver biochemistries will be diagnosed with "idiopathic neonatal hepatitis." Understanding that the best therapeutic interventions are those that target key mechanisms of injury, it is paramount to continue to investigate the biological, molecular, genetic, and cellular contributions to this devastating disease to enable better treatment strategies that will change the outcome for affected children.

James E. Squires, MD, MS
Division of Gastroenterology
Advanced Hepatology
Cincinnati Children's Hospital Medical Center
Cincinnati, Ohio

http://dx.doi.org/10.1016/j.jpeds.2014.06.006

References

1. Balistreri WF. Growth and development of a new subspecialty: pediatric hepatology. Hepatology 2013;58:458-76.
2. Alagille D, Thomassin HE. L'atresie des voies biliares intrahepatiques avec voies biliaires extrahepatiques permeables chez l'enfant. Ann Med Interne (Paris) 1972;123:871-3.

PEDIATRICS INTERNATIONAL Official Journal of the Japan Pediatric Society

Pediatrics International (2014) **56**, 506–509 doi: 10.1111/ped.12439

Review Article

Diagnosis and treatment of urea cycle disorder in Japan

Kimitoshi Nakamura,[1] Jun Kido,[1] Hiroshi Mitsubuchi[2] and Fumio Endo[1]

Departments of [1]Pediatrics and [2]Neonatology, Kumamoto University Hospital, Kumamoto, Japan

Abstract Urea cycle disorder (UCD) is an inborn error of the metabolic pathway producing urea from ammonia, which occurs primarily in the liver. Decreased excretion of nitrogen in the urea cycle due to deficiency of carbamoyl phosphate synthase I (CPSI), ornithine transcarbamylase (OTC), argininosuccinate synthase (ASS), argininosuccinate lyase (ASL), and *N*-acetyl glutamate synthase (NAGS) causes hyperammonemia. We examined the clinical manifestations, treatment, and prognosis of 177 patients with UCD from January 1999 to March 2009 in Japan. Compared with a previous study conducted in Japan, a larger number of patients survived without mental retardation, even when the peak blood ammonia was >360 μmol/L. In those with peak blood ammonia >360 μmol/L, an indicator of poor prognosis, the frequency of convulsions, mental retardation, brain abnormality on magnetic resonance imaging, hemodialysis, liver transplantation, and intake of non-protein formulas was significantly higher than in those with peak blood ammonia <360 μmol/L. In this article, we have reported the current state of UCD to evaluate prognosis and its relationship with peak blood ammonia and hemodialysis.

Key words carbamoyl phosphate synthase I deficiency, hemodialysis, hyperammonemia, liver transplantation, ornithine transcarbamylase deficiency.

The urea cycle is a pathway by which urea is produced from ammonia primarily in the liver (Fig. 1).[1] It is composed of four amino acids, namely ornithine, citrulline, argininosuccinic acid, and arginine. Citrulline is composed of ornithine and carbamoyl phosphate, and argininosuccinic acid is composed of citrulline and aspartic acid. Argininosuccinic acid is decomposed into fumaric acid and arginine, and arginine is disassembled into ornithine and urea. Ammonia is detoxified during the urea cycle to produce urea. Two nitrogen atoms in urea originate from aspartic acid and carbamoyl phosphate. Urea cycle disorder (UCD) is an inborn error of this metabolic pathway. Decreased excretion of nitrogen in the urea cycle due to deficiency of carbamoyl phosphate synthase (CPSI), ornithine transcarbamylase (OTC), argininosuccinate synthase (ASS), argininosuccinate lyase (ASL), arginase (ARG) and *N*-acetyl glutamate synthase (NAGS) causes hyperammonemia.[1–3] Additionally, *N*-acetyl glutamic acid is essential to the activity of CPSI. Decrease in *N*-acetyl glutamic acid secondary to abnormality of NAGS results in UCD, which causes hyperammonemia. CPSI and OTC are found in the mitochondria, and other enzymes are located outside of it. In citrin deficiency and lysinuric protein intolerance, the activity of the urea cycle decreases to cause hyperammonemia.

There are many reports on the long-term prognosis of UCD patients in Japan and other countries,[3–12] including one by us on long-term prognosis and treatment of UCD patients.[13] As with the previous studies, we found that the prognosis and neurological symptoms of UCD patients improved with early treatment. Furthermore, hemodialysis was performed in UCD patients with high peak blood ammonia at onset. In this study, we investigated the current state of UCD to evaluate the prognosis and its relationship with peak blood ammonia and hemodialysis.[13,14]

This study was approved by the ethics committee of the Faculty of Life Science, Kumamoto University.

Correspondence: Kimitoshi Nakamura, MD, PhD, Department of Pediatrics, Kumamoto University Hospital, Honjo 1-1-1, Chuo-ku, Kumamoto 860-8556, Japan. Email: nakamura@kumamoto-u.ac.jp

Received 13 May 2014; accepted 17 June 2014.

Epidemiology

The incidence, time of onset, and survival rate for the different types of UCD are listed in Table 1.[13] Among these, OTC deficiency is the most common and accounts for approximately two-thirds of the total incidence.[6,8] OTC deficiency involves X chromosome-linked inheritance. An equal number of women and men are affected by this disorder. CPSI deficiency, citrullinemia type I comprised >10% of UCD, respectively, and only one argininemia was found.[13] During the newborn period, 75–90% of UCD patients who died had CPSI deficiency, citrullinemia type I, argininosuccinic aciduria, whereas many late-onset patients who died had OTC deficiency. The survival rate for the neonatal-onset type was 75–90% and that of the late-onset type was approximately ≥90%. The survival rate of the OTC deficiency type was 90% in men and 88% in women; this was lower than the survival rate for other UCD.

Clinical manifestations

Blood ammonia concentration is maintained at 10–40 μmol/L in healthy individuals.[1,2,15] Ammonia >60 μmol/L causes symptoms such as anorexia, nausea, excitement, insomnia, and character

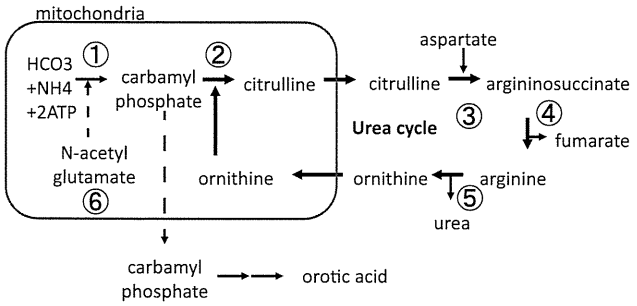

Fig. 1 Urea cycle and its enzymes: 1, carbamoyl phosphate synthase; 2, ornithine transcarbamylase; 3, argininosuccinate synthase; 4, argininosuccinate lyase; 5, arginase; and 6, *N*-acetyl glutamate synthase.

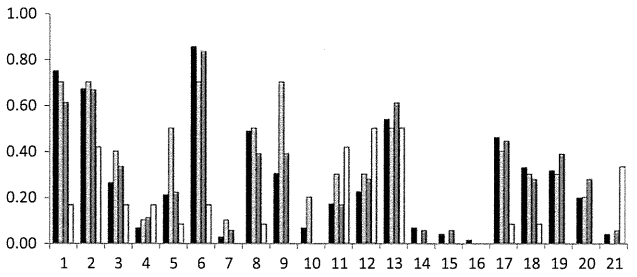

Fig. 2 Incidence of clinical symptoms in urea cycle disorder: 1, nausea and vomiting; 2, loss of appetite; 3, failure to thrive; 4, hypoglycemia; 5, acidemia; 6, hyperammonemia; 7, hyperuricemia; 8, convulsion; 9, mental retardation; 10, visual disturbance; 11, hepatomegaly; 12, fatty liver; 13, liver failure; 14, renal failure; 15, heart disorder; 16, increased susceptibility to infection; 17, abnormal brain magnetic resonance imaging and/or computed tomography; 18, abnormal electroencephalogram; 19, hemodialysis; 20, peritoneal dialysis; 21, other. ■, ornithine transcarbamylase deficiency; ▨, carbamoyl-phosphate synthetase 1 deficiency; ▩, argininosuccinate synthase deficiency; □, citrin deficiency.

change.[1] Because the neonatal liver is premature, the ammonia level may rise up to 120 μmol/L even in those without UCD; careful attention is therefore necessary for diagnosis.[1] Convulsions and disturbance of consciousness may develop when blood ammonia increases to >120 μmol/L. When the ammonia level exceeds 240 μmol/L, the patient may develop coma and respiratory depression.[2,15] Frequency of clinical manifestations has been evaluated in OTC deficiency, CPSI deficiency, citrullinemia type I, and citrin deficiency (Fig. 2). Frequently occurring symptoms are as follows: nausea and vomiting, loss of appetite, acidemia, failure to thrive, hyperammonemia, convulsions, abnormal brain magnetic resonance imaging and/or computed tomography, liver failure, fatty liver, hepatomegaly, and mental retardation. In general, central nervous system involvement becomes irreversible with a continuing rise of ammonia level.[9] Severity of the disorder is associated with the duration of peak ammonia at onset. Therefore, psychomotor developmental delay may persist even if hyperammonemia is improved. Immediate initiation of treatment for hyperammonemia is important. The relationship between highest blood ammonia concentration at onset and prognosis is shown in Figure 3.[12,13] Prognosis is remarkably poor when blood ammonia is ≥360 μmol/L. The prognosis of UCD improved in 1999–2009[13] compared to that in 1975–1995,[12] and there has been further improvement in prognosis in recent years.

Laboratory studies

Urea cycle disorder is suspected when the blood ammonia level is higher than the standard level of 60 μmol/L.[1,2,8,15] In most cases of UCD of neonatal onset, blood ammonia is >120 μmol/L. It is not unusual for this level to increase to >600 μmol/L at onset. The presence of liver damage is evaluated on a general biochemistry test. There are many cases of a slight elevation of aspartate aminotransferase, alanine aminotransferase, and decrease of blood urea nitrogen (BUN). UCD patients do not usually present with acidosis, but they sometimes present with secondary metabolic acidosis when in a state of shock and convulsions. Citrullinemia, argininosuccinic aciduria, and argininemia are usually diagnosed on blood and urinary amino acid analysis. When blood citrulline is low, OTC deficiency and CPSI deficiency are suspected.[1] If low blood lysine and arginine are found, lysinuric protein intolerance is suspected. For the diagnosis of OTC and CPSI deficiencies, urinary organic acid analysis is important to evaluate the elevation of urinary orotic acid.[6] The diagnosis of OTC deficiency in a heterozygote female patient is

Table 1 Type of UCD in Japan vs onset and survival

	Total	Onset time			Surviving patients	
		Neonatal onset	Late onset	Unknown	Nenonatal onset	Late onset
Male OTCD	57 (32)	21 (37)	30 (53)	6 (10)†	17 (81)	27 (90)
Female OTCD	59 (33)	7 (12)	50 (85)	2 (3)	6 (86)	44 (88)
CPSD	23 (13)	19 (83)	3 (13)	1 (4)	15 (79)	3 (100)
ASD	28 (16)	21 (75)	7 (25)	0	19 (90)	7 (100)
ALD	9 (5)	8 (89)	1 (11)	0	6 (75)	1 (100)
AGD	1 (0.6)	1 (100)	0	0	1 (100)	0
Total	177 (100)	77 (44)	91 (51)	9 (5)‡	64 (83)	82 (90)

Neonatal onset, ≤28 days from birth; late onset, >28 days after birth. †Includes one patient treated before manifestation of symptoms and five patients for whom onset timing was unknown. ‡Includes one patient treated before manifestation of symptoms and eight patients in whom onset timing was unknown. AGD, arginase-1 deficiency; ALD, argininosuccinate lyase deficiency; ASD, argininosuccinate synthetase deficiency; CPSD, carbamoyl-phosphate synthetase 1 deficiency; OTCD, ornithine transcarbamylase deficiency; UCD, urea cycle disorder.

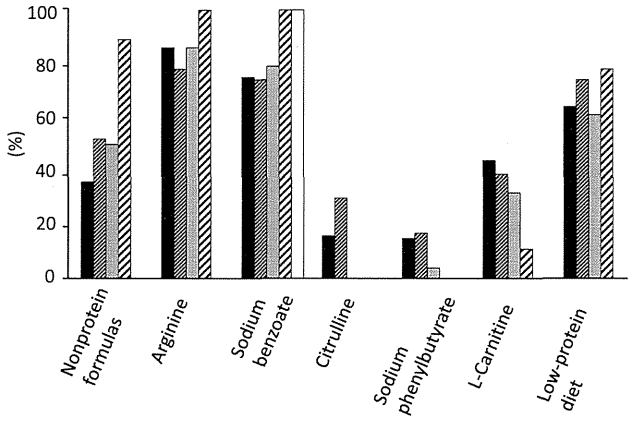

Fig. 3 Therapy frequently used for urea cycle disorder in Japan. Arginine and sodium benzoate are frequently used. The use of citrulline is recommended for ornithine transcarbamylase deficiency (OTCD) and carbamoyl-phosphate synthetase 1 deficiency (CPSD). Apart from being expensive, citrulline, sodium benzoate and sodium phenylbutyrate were not government-approved drugs in Japan, and, therefore, patients had to pay for them. Less than 75% of patients with CPSD and argininosuccinate synthetase deficiency (ASD) were treated with a low-protein diet. ■, OTCD; ▨, CPSD; ▨, ASD; ▨, argininosuccinate lyase deficiency; □, arginase-1 deficiency.

sometimes difficult and allopurinol loading test is needed to evaluate orotic acid for diagnosis. Confirmed diagnosis may require enzyme and/or gene analysis.

Because it is limited to the site where the enzyme is found, the organ available for enzyme diagnosis requires careful attention for the specimen sampling.

Treatment

Treatment of UCD is divided into two phases: acute and chronic.[10,15] Acute exacerbation should be prevented as much as possible and treated immediately in the event of occurrence. Blood ammonia should be maintained within the normal range and good developmental growth should be maintained during the chronic phase. Treatment of UCD as currently performed in Japan is shown in Figure 3.[13] In most cases, arginine and sodium benzoate are given, and a low-protein diet is supplied.[16–21] Only a few patients were given citrulline and sodium phenylbutyrate because in 2007 citrulline was registered as a food and not as a medicine. Sodium phenylbutyrate was registered as medicine in 2013. Citrulline for UCD patients is supplied by the Japanese Society for Inherited Metabolic Disease from 2010. Use of these for treatment is increasing.

Treatment of the acute phase

In the acute phase, first the blood ammonia should be decreased. Sufficient infusion (60–100 kcal/kg per day) of glucose electrolyte solution should be carried out to inhibit protein catabolism.[10] Insulin should be used simultaneously in cases of hyperglycemia. Arginine should be used for UCD other than argininemia. Citrulline is effective for OTC deficiency and CPSI deficiency and is thought to be more effective than arginine. Sodium benzoate and sodium phenyl butyrate should be used for excretion of excess nitrogen. The ammonia level may decrease within several hours, but, if 8 h later ammonia is >360 μg/dL, hemodialysis or hemofiltration dialysis should be started immediately.[13,22] Ammonia removal efficiency by exchange blood transfusion and by peritoneal dialysis is poor, and transportation of the patient to a special metabolic facility for hemodialysis or hemofiltration dialysis should be considered. After decreasing the blood ammonia level, oral intake should be considered with increasing essential amino acids while adjusting the total energy and protein intake with a protein removal formula (S-23). The treatment should aim for an intake of total protein 1.0–1.2 g/kg per day with spontaneous protein and required amino acid preparation.

Treatment of the chronic phase

Diet, amino acid intake, and drugs are essential for treatment in the chronic phase. For OTC and CPSI deficiency, protein intake should be restricted to 1.25–1.75 g/kg per day and, for ASS deficiency and ASL deficiency, it should be restricted to 1.75 g/kg per day.[1,5,10,15] Adjustment of this restriction based on residual enzyme activity is necessary. Treatment with essential amino acids is necessary during protein restriction. Therapy using carbamoyl glutamine is attempted for NAGS and CPSI deficiencies. Regular checks to assess height and weight gain, ammonia concentration in blood, amino acids (glutamine, arginine, citrulline, glycine, other essential amino acids), transaminase, BUN, and electrolytes is necessary for treatment evaluation. Imaging of the liver and head should be considered. Ammonia should be maintained at ≤150 μg/dL, glutamine at ≤1000 μmol/L, and arginine at 80–150 μmol/L. Liver transplantation has recently been performed safely in patients with inherited metabolic disease.

Liver transplantation is indicated in moderate–severe UCD.[23,24] The transplantation should be performed after encephalopathy due to hyperammonemia at onset is minimal, and before subsequent acute aggravation. Female patients with OTC deficiency should also be considered for liver transplantation.

Complications and prognosis

Hyperammonemia can cause central nervous system disturbance. Initial presentation at the acute stage manifests as absentmindedness, nausea, and feeling ill. Early identification of UCD symptoms is important. Treatment complications such as dermatitis, and skin rash due to protein insufficiency, alopecia, and fatty liver are often observed.[1,2] Additionally, it can lead to deficiency in iron, trace elements, and vitamins. Supplementation is therefore necessary. The present prognosis of UCD is greatly improved compared to that in the past (Fig. 4). One of the reasons for this improvement is aggressive therapy with hemodialysis or hemofiltration dialysis, performed in an institution that specializes in this treatment. Neonatal onset of OTC and CPSI deficiencies, however, causes many fatalities. In heterozygote women with OTC deficiency, acute aggravation can occur in the long term and may be life-threatening. A poor prognosis and serious sequelae are associated with the highest ammonia blood concentration at onset. The prognosis in 2012 has been reported as

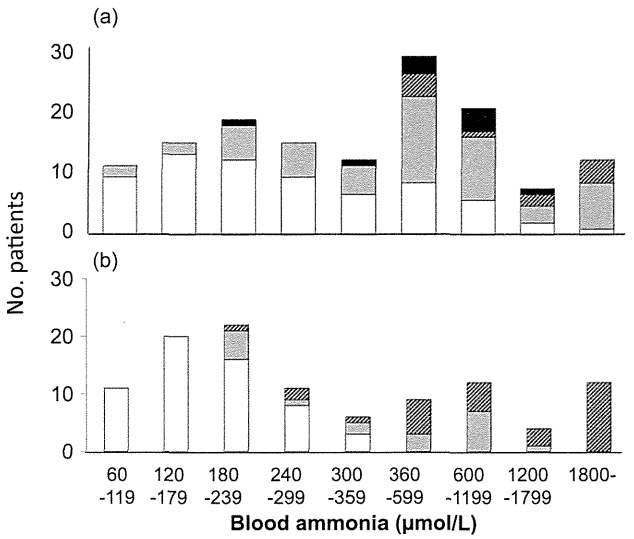

Fig. 4 Relationship between peak blood ammonia levels and neurodevelopmental outcome: (a) Kido *et al.* (2012);[13] (b) Uchino *et al.* (1998).[12] Eighteen urea cycle disorder patients with maximum ammonia concentration >360 μmol/l had normal neurodevelopment. ■, unknown; ▨, deceased; ▤, mentally handicapped; □, normal.

improved with a survival rate of 80–90%, 20 years after onset,[13] compared to a previously reported rate of 20–40% in 1998.[12] The prognosis could be favorable if the hyperammonemia is treated immediately and aggressively. It is important for this treatment to be performed in association with an institution that specializes in this treatment.

Acknowledgments

The work was supported by a Grant-in-Aid from the Ministry of Health, Labour and Welfare of Japan. We thank Dr Reiko Horikawa and Dr Mureo Kasahara from the National Center for Child Health and Development, Dr Toshihiro Ohura from Sendai City Hospital, Dr Masaki Takayanagi from Chiba Children's Hospital, Dr Masafumi Matsuo from Kobe University, Dr Makoto Yoshino from Kurume University, Dr Yosuke Shigematsu from University of Fukui, and Dr Tohru Yorifuji from Osaka City General Hospital for useful discussions and information.

References

1 Brusilow SW, Horwich AL. Urea cycle enzymes. In: Scriver CR, Beaudet AL, Sly WS, Valle D (eds). *The Metabolic and Molecular Bases of Inherited Disease*, 8th edn. McGraw-Hill, New York, 2001; 1909–63.
2 Endo F, Matsuura T, Yanagida K *et al.* Clinical manifestation of inborn errors of urea cycle and related metabolic disorders during childhood. *J. Nutr.* 2004; **134**: 1605S–9S.
3 Nagata N, Matsuda I, Oyanagi K. Estimated frequency of urea cycle enzymopathies in Japan. *Am. J. Med. Genet.* 1991; **39**: 228–9.
4 Matsuda I, Tanase S. The ornithine transcarbamylase (OTC) gene: Mutations in 50 Japanese families with OTC deficiency. *Am. J. Med. Genet.* 1997; **71**: 378–83.
5 Bachmann C. Outcome and survival of 88 patients with urea cycle disorders: A retrospective evaluation. *Eur. J. Pediatr.* 2003; **162**: 410–16.
6 Maestri NE, Brusilow SW, Clissold DW, Bassett SS. Long-term treatment of girls with ornithine transcarbamylase deficiency. *N. Engl. J. Med.* 1996; **335**: 855–9.
7 Matsuda I, Nagata N, Matsuura T *et al.* Retrospective survey of urea cycle disorders: Part 1. Clinical and laboratory observations of thirty-two Japanese male patients with ornithine transcarbamylase deficiency. *Am. J. Med. Genet.* 1991; **38**: 85–9.
8 Msall M, Batshaw ML, Suss R, Brusilow SW, Mellits SD. Neurological outcome in children with inborn errors of urea synthesis. Outcome of urea-cycle enzymopathies. *N. Engl. J. Med.* 1984; **310**: 1500–5.
9 Nagata N, Matsuda I, Matsuura T *et al.* Retrospective survey of urea cycle disorders: Part 2. Neurological outcome in forty-nine Japanese patients with urea cycle enzymopathies. *Am. J. Med. Genet.* 1991; **40**: 477–81.
10 Nassogne MC, Héron B, Touati G, Rabier D, Saudubray JM. Urea cycle defects: Management and outcome. *J. Inherit. Metab. Dis.* 2005; **28**: 407–14.
11 Nicolaides P, Liebsch D, Dale N, Leonard J, Surtees R. Neurological outcome of patients with ornithine carbamoyltransferase deficiency. *Arch. Dis. Child.* 2002; **86**: 54–6.
12 Uchino T, Endo F, Matsuda I. Neurodevelopmental outcome of long-term therapy of urea cycle disorders in Japan. *J. Inherit. Metab. Dis.* 1998; **21**: 151–9.
13 Kido J, Nakamura K, Mitsubuchi H *et al.* Long-term outcome and intervention of urea cycle disorders in Japan. *J. Inherit. Metab. Dis.* 2012; **35**: 777–85.
14 Kido J, Nakamura K, Matsumoto S *et al.* Current status of hepatic glycogen storage disease in Japan: Clinical manifestations, treatments and long-term outcomes. *J. Hum. Genet.* 2013; **58**: 285–92.
15 Summar M. Current strategies for the management of neonatal urea cycle disorders. *J. Pediatr.* 2001; **138**: S30–39.
16 Brusilow SW, Valle DL, Batshaw M. New pathways of nitrogen excretion in inborn errors of urea synthesis. *Lancet* 1979; **2**: 452–4.
17 Brusilow SW. Phenylacetylglutamine may replace urea as a vehicle for waste nitrogen excretion. *Pediatr. Res.* 1991; **29**: 147–50.
18 Nagasaka H, Yorifuji T, Murayama K *et al.* Effects of arginine treatment on nutrition, growth and urea cycle function in seven Japanese boys with late-onset ornithine transcarbamylase deficiency. *Eur. J. Pediatr.* 2006; **165**: 618–24.
19 Leonard JV. The nutritional management of urea cycle disorders. *J. Pediatr.* 2001; **138**: S40–S44.
20 Feillet F, Leonard JV. Alternative pathway therapy for urea cycle disorders. *J. Inherit. Metab. Dis.* 1998; **21**: 101–11.
21 Batshaw ML, MacArthur RB, Tuchman M. Alternative pathway therapy for urea cycle disorders: Twenty years later. *J. Pediatr.* 2001; **138**: S46–S54.
22 Schaefer F, Straube E, Oh J, Mehls O, Mayatepek E. Dialysis in neonates with inborn errors of metabolism. *Nephrol. Dial. Transplant.* 1999; **14**: 910–18.
23 Uemoto S, Yabe S, Inomata S *et al.* Coexistence of a graft with the preserved native liver in auxiliary partial orthotopic liver transplantation from a living donor for ornithine transcarbamylase deficiency. *Transplantation* 1997; **63**: 1026–8.
24 Morioka D, Kasahara M, Takada Y *et al.* Current role of liver transplantation for the treatment of urea cycle disorder: A review of the worldwide English literature and 13 cases at Kyoto University. *Liver Transpl.* 2005; **11**: 1332–42.

RESEARCH ARTICLE

AMERICAN JOURNAL OF medical genetics PART A

Mutations in *HADHB*, which Encodes the β-Subunit of Mitochondrial Trifunctional Protein, Cause Infantile Onset Hypoparathyroidism and Peripheral Polyneuropathy

Misako Naiki,[1,2] Nobuhiko Ochi,[3] Yusuke S. Kato,[4] Jamiyan Purevsuren,[5] Kenichiro Yamada,[1] Reiko Kimura,[1] Daisuke Fukushi,[1] Shinya Hara,[6] Yasukazu Yamada,[1] Toshiyuki Kumagai,[7] Seiji Yamaguchi,[5] and Nobuaki Wakamatsu[1]*

[1]Department of Genetics, Institute for Developmental Research, Aichi Human Service Center, Kasugai, Aichi, Japan

[2]Department of Pediatrics, Nagoya University Graduate School of Medicine, Nagoya, Aichi, Japan

[3]Department of Pediatrics, Daini-Aoitori Gakuen, Aichi Prefectural Hospital and Habilitation Center for Disabled Children, Okazaki, Aichi, Japan

[4]Institute for Health Science, Tokushima Bunri University, Tokushima, Japan

[5]Department of Pediatrics, Shimane University, Faculty of Medicine, Izumo, Shimane, Japan

[6]Department of Pediatrics, Toyota Memorial Hospital, Toyota, Aichi, Japan

[7]Department of Pediatric Neurology, Kobato Gakuen, Aichi Human Service Center, Kasugai, Aichi, Japan

Manuscript Received: 18 July 2013; Manuscript Accepted: 16 December 2013

Mitochondrial trifunctional protein (MTP) is a hetero-octamer composed of four α- and four β-subunits that catalyzes the final three steps of mitochondrial β-oxidation of long chain fatty acids. *HADHA* and *HADHB* encode the α-subunit and the β-subunit of MTP, respectively. To date, only two cases with MTP deficiency have been reported to be associated with hypoparathyroidism and peripheral polyneuropathy. Here, we report on two siblings with autosomal recessive infantile onset hypoparathyroidism, peripheral polyneuropathy, and rhabdomyolysis. Sequence analysis of *HADHA* and *HADHB* in both siblings shows that they were homozygous for a mutation in exon 14 of *HADHB* (c.1175C>T, [p.A392V]) and the parents were heterozygous for the mutation. Biochemical analysis revealed that the patients had MTP deficiency. Structural analysis indicated that the A392V mutation identified in this study and the N389D mutation previously reported to be associated with hypoparathyroidism are both located near the active site of MTP and affect the conformation of the β-subunit. Thus, the present patients are the second and third cases of MTP deficiency associated with missense *HADHB* mutation and infantile onset hypoparathyroidism. Since MTP deficiency is a treatable disease, MTP deficiency should be considered when patients have hypoparathyroidism as the initial presenting feature in infancy.

Key words: hypoparathyroidism; MTP deficiency; HADHB; LCKT; peripheral polyneuropathy

How to Cite this Article:
Naiki M, Ochi N, Kato YS, Purevsuren J, Yamada K, Kimura R, Fukushi D, Hara S, Yamada Y, Kumagai T, Yamaguchi S, Wakamatsu N. 2014. Mutations in *HADHB*, which encodes the β-subunit of mitochondrial trifunctional protein, cause infantile onset hypoparathyroidism and peripheral polyneuropathy.
Am J Med Genet Part A 164A:1180–1187.

Conflict of Interest: The authors declare no conflict of interests.
Grant sponsor: Takeda Science Foundation; Grant sponsor: Health Labor Sciences Research Grant; Grant sponsor: Ministry of Education, Culture, Sports, Science, and Technology of Japan (to N.W.); Grant number: #21390319.

Abbreviations: MTP, mitochondrial trifunctional protein; PTH, parathyroid hormone; LCEH, long-chain enoyl-CoA hydratase; LCHAD, long-chain 3-hydroxyacyl-CoA dehydrogenase; LCKT, long-chain 3-ketoacyl-CoA thiolase; CMT, Charcot-Marie-Tooth; MCAD, medium-chain acyl-CoA dehydrogenase.

*Correspondence to:
Nobuaki Wakamatsu, M.D., Ph.D., Department of Genetics, Institute for Developmental Research, Aichi Human Service Center, 713-8 Kamiya-cho, Kasugai, Aichi 480-0392, Japan.
E-mail: nwaka@inst-hsc.jp

Article first published online in Wiley Online Library (wileyonlinelibrary.com): 24 March 2014
DOI 10.1002/ajmg.a.36434

INTRODUCTION

MTP is a hetero-octamer composed of four α- and four β-subunits and contains three different enzyme activities that catalyze the final three chain-shortening reactions in the β-oxidation of long-chain fatty acids [Uchida et al., 1992]. *HADHA* encodes the α-subunit, which has both long-chain enoyl-CoA hydratase (LCEH, EC 4.2.1.17) and long-chain 3-hydroxyacyl-CoA dehydrogenase (LCHAD, EC 1.1.1.211) activities, whereas *HADHB* encodes the β-subunit, which has only long-chain 3-ketoacyl-CoA thiolase (LCKT, EC 2.3.1.16) activity [Uchida et al., 1992]. Mutations in *HADHA* or *HADHB* cause MTP (LCEH, LCHAD, LCKT) deficiency, with decreased activity and levels of all three enzymes because of the failure of hetero-octamer formation; however, a homozygous mutation (1528G>C) in *HADHA* has been reported to cause an isolated LCHAD deficiency [IJlst et al., 1994]. MTP deficiency is characterized by a wide range of clinical features, including cardiomyopathy, hypoketonic hypoglycemia, metabolic acidosis, sudden infant death, metabolic encephalopathy, liver dysfunction, peripheral neuropathy, exercise-induced myoglobinuria, and rhabdomyolysis [Wanders et al., 1999].

Hypoparathyroidism is a rare disorder characterized by hypocalcemia and hyperphosphatemia and is caused by deficiency in parathyroid hormone (PTH) action. An epidemiological survey showed that the prevalence of idiopathic hypoparathyroidism in Japan is 1:140,000 [Nakamura et al., 2000]. Impaired secretion of PTH causes PTH-deficient hypoparathyroidism, while resistance to PTH due to a defect in the PTH receptor or insensitivity to PTH results in pseudohypoparathyroidism. Autosomal recessive forms of isolated hypoparathyroidism have been reported to be caused by mutations in *PTH*, located on chromosome 11p15 [Parkinson and Thakker, 1992] or the gene encoding the parathyroid-specific transcription factor glial cells missing B (*GCMB*) on 6p24 [Ding et al., 2001].

Here, we report that two siblings born to consanguineous parents have MTP deficiency associated with infantile onset hypoparathyroidism. We have identified a new missense mutation in *HADHB* located close to the active site of the β-subunit of MTP. We also review hypoparathyroidism caused by MTP deficiencies and discuss the pathogenesis of the disease associated with hypoparathyroidism.

PATIENTS AND METHODS

Written informed consent was obtained from the patients and the family members who participated in this study. The experiments were conducted after approval by the institutional review board at the Institute for Developmental Research, Aichi Human Service Center.

The proband (IV-1) is an 18-year-old female born to first-cousin parents as a dizygotic twin (Fig. 1A). She was born at 37 weeks and 4 days gestation by normal vaginal delivery following an uneventful pregnancy. She was hospitalized 5 weeks after birth because of generalized seizures. Biochemical analysis revealed a decreased serum calcium concentration of 1.15 mmol/L (normal range: 2.25–2.75 mmol/L) and an elevated serum phosphorus concentration of 3.49 mmol/L (normal range: 1.21–2.18 mmol/L). The serum concentration of intact-PTH (iPTH) was below detectable levels (<5 pg/ml; normal range: 10–65 pg/ml). The concentrations of serum creatinine and blood urea nitrogen (BUN) were 0.3 mg/dl (normal range: 0.1–0.4 mg/dl) and 7 mg/dl (normal range: 7–19 mg/dl), respectively; thus, renal function was normal. She was diagnosed with hypoparathyroidism and was treated with activated vitamin D and calcium. The therapy elevated the serum calcium concentration, and she no longer experienced seizures. At 1 year of age, her serum calcium concentration had increased to 2.00 mmol/L, but her serum iPTH concentration was undetectable (<5 pg/ml). She achieved all developmental milestones at the appropriate age. At 2 years, she was admitted to the hospital with tetany after an upper respiratory tract infection. Upon admission, laboratory examination revealed an elevated serum creatine kinase concentration of 9,577 U/L (normal range: 20–150 U/L) and a low serum calcium concentration of 1.48 mmol/L. She was diagnosed with rhabdomyolysis and hypocalcemia and was successfully treated with intravenous fluids. She was later admitted to the hospital with recurrent episodes of fever, hypocalcemia, rhabdomyolysis, and myoglobinuria for several years. She has also experienced distal lower limb muscle weakness and atrophy since 3 years of age. Because of having a drop foot, she has had difficulty walking and has used foot orthoses or a wheelchair since she was 9. A neurologic examination at 9 years of age demonstrated distal muscle weakness, particularly involving the peroneal muscles, with absent tendon reflexes. There were no signs of pyramidal tract involvement. The motor conduction velocity of the peroneal nerve was decreased to 21.6 m/sec (normal range: 40–65 m/sec). Sensory conduction velocity of the sural nerve could not be evoked. The Gower's sign was negative. Thus, she has peripheral sensorimotor polyneuropathy. A muscle biopsy from the left biceps brachii demonstrated denervation atrophy with a predominance of type I fibers. She currently presents with severe muscular atrophy of the lower legs and hands with an absence of Achilles and patellar tendon reflexes, which are the clinical features of Charcot-Marie-Tooth (CMT) disease. She also has a drop foot and hammer toes, and touch and vibration senses of the distal legs are diminished (Fig. 1B). The serum calcium and iPTH concentrations at present were 2.10 mmol/L and 5 pg/ml, respectively. Analysis of blood acylcarnitines and urine organic acids measured once in a non-acute phase showed no abnormalities.

Patient IV-2 is an 18-year-old male who is the dizygotic twin of Patient IV-1 (Fig. 1A). Because his twin sister had hypoparathyroidism at the age of 1 month, his serum concentration of iPTH was measured at 4 months. He was asymptomatic, but his serum iPTH concentration was undetectable (<5 pg/ml) with a decreased calcium concentration (1.50 mmol/L) and an elevated phosphorus concentration (3.97 mmol/L). He started a regimen of activated vitamin D and calcium. He did not experience seizures but developed progressive peripheral polyneuropathy, and has exhibited rhabdomyolysis triggered by fevers from viral infections since he was 3. At 9 years of age, the motor conduction velocity of the peroneal nerve was decreased to 35.6 m/sec, and sensory conduction velocity of the sural nerve was not evoked. Findings from a muscle biopsy performed at 10 years of age were similar to those obtained for his sister. At 10 years of age, he required ventilator support owing to respiratory failure following an episode of rhab-

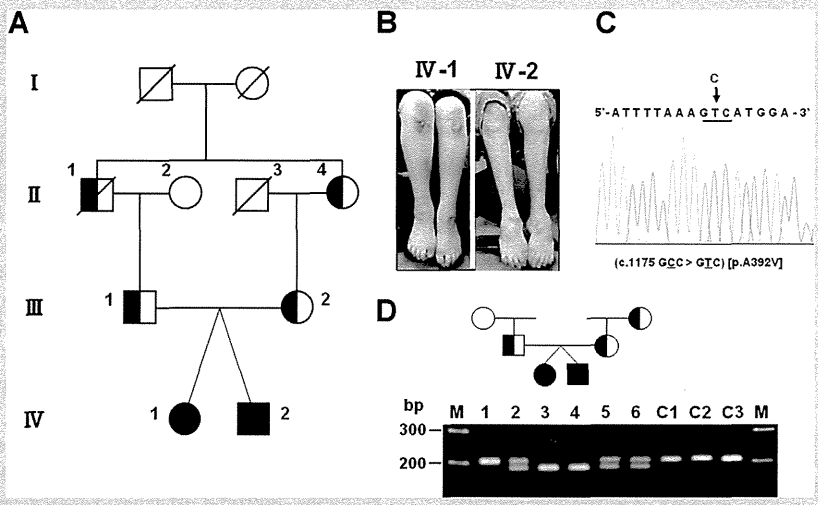

FIG. 1. The identification of the mutation in *HADHB*. A: The pedigree of the family with hypoparathyroidism and peripheral polyneuropathy. Affected individuals are indicated by filled symbols, unaffected individuals by unfilled symbols, and carrier individuals by half-filled symbols. B: The patients have muscle atrophy of the lower legs and deformity of the toes [hammer toes]. C: The direct sequence analysis of the patient IV-1 revealed a C to T substitution at nucleotide position 1175 in exon 14 of *HADHB*, resulting in the substitution of alanine [GCC] at codon 392 with valine [GTC] [c.1175C>T, [p.Ala392Val]], as indicated by the arrow. D: PCR-RFLP analysis using *Bsp*HI-digested PCR products from family members and three normal controls [C1, C2, and C3] were run through a 1.5% low-melting agarose gel. The sizes of the DNA markers are indicated on the left side.

domyolysis and myoglobinuria with a decreased calcium concentration (1.88 mmol/L) and a normal phosphorus concentration (1.93 mmol/L); however, his renal function was normal, as indicated by his serum creatinine (0.3 mg/dl) and BUN (17 mg/dl) concentrations. Analysis of blood acylcarnitines and urine organic acids in a non-acute phase showed no abnormalities. The serum calcium and iPTH concentrations at present were 2.20 mmol/L and 6 pg/ml, respectively. He currently presents with clinical features similar to those of his sister (Fig. 1B).

Patient IV-1 developed seizures due to hypoparathyroidism at 5 weeks after birth, and hypoparathyroidism was diagnosed in Patient IV-2 at the age of 4 months. Thus, both patients presented with infantile onset hypoparathyroidism. The clinical features of the presented patients are summarized in Table I.

DNA Analysis

Genomic DNA was isolated from white blood cells by phenol/chloroform extraction. Specific primers were designed to amplify *PTH*, *GCMB*, *HADHA*, and *HADHB*. PCR-amplified DNA fragments were isolated, purified, and sequenced using the Big Dye Terminator Cycle Sequencing Kit (Applied Biosystems, Foster City,

TABLE I. Clinical and Molecular Features of Hypoparathyroidism Associated With MTP Deficiency

Patients	**1**	**2**	**3**	**4**
Gender	Female	Female	Female	Male
Age at onset				
Hypoparathyroidism	15 m	4 m	5 w	4 m
Rhabdomyolysis	15 m	15 m	2 y	3 y
Peripheral polyneuropathy	15 m	4 m	3 y	3 y
Hypotonia	+	+	−	−
Liver dysfunction	+	+	−	−
HADHA/HADHB mutation	ND	N389D (HADHB)	A392V (HADHB)	A392V (HADHB)
References	Dionisi-Vici et al. [1996]	Labarthe et al. [2006]	This study	This study

+, present; −, not present; ND, not described; w, week; m, month; y, year.

CA). Mismatch primer pairs (sense: 5′-tgctgggattacagatgtgag-3′; antisense: 5′-tgcaaaccaatcagaattcatg-3′) were prepared for PCR-RFLP analysis to generate the *Bsp*HI site (tcatga) in a mutant allele. *Bsp*HI was used to digest the 200-bp mutant (c.1175C>T) PCR product, which generated the 178-bp PCR product.

Enzyme Assay

Mitochondrial LCKT activity in lymphoblastoid cells from the two patients and from two healthy adult males (as the control) was determined using 10 μM 2-ketopalmitoyl-CoA as a substrate [Purevsuren et al., 2009]. Citrate synthase activity was determined spectrophotometrically using DTNB.

MTP Expression Analysis

Cell extracts of lymphoblastoid cells from Patients IV-1 and IV-2 and two healthy adult males and of MTP-deficient fibroblasts (previously reported by Purevsuren et al. [2009]) were subjected to 12.5% sodium dodecyl sulfate-polyacrylamide gel electrophoresis (SDS-PAGE). Western blot analysis was performed using a rabbit polyclonal antibody specific for both the α- and β-subunits of MTP or medium-chain acyl-CoA dehydrogenase (MCAD) (both antibodies were generously provided by Dr. T. Hashimoto, Professor Emeritus, Shinshu University), and blots were visualized using the Immuno-Pure NBT/BCIP Substrate Kit (Promega, Madison, WI).

Construction of Wild-Type and Mutant HADHB-FLAG and Wild-Type HADHA-MYC Expression Vectors

The wild-type HADHB expression vector was prepared by subcloning *HADHB* cDNA at the *Not*I/*Eco*RV site of a mammalian expression vector, p3 × FLAG-CMV (Sigma–Aldrich, St. Louis, MO) (pHADHB-FLAG). An *Eco*RV recognition site (gatatc) was introduced at the termination codon (TAA) of *HADHB*. The mutant *HADHB* (pHADHB-A392V-FLAG, pHADHB-R61C-FLAG, pHADHB-N389D-FLAG, and pHADHB-R444K-FLAG; amino acid number is shown from the first methionine) and the wild-type *HADHA* (pHADHA-MYC) expression vectors were prepared using the in vitro mutagenesis method [Yamada et al., 2013]. The generated expression vectors encoded the FLAG-tagged wild-type or mutant β-subunits and MYC-tagged α-subunit protein at the *C*-terminus.

Analysis of the Association of the Wild-Type or Mutant β-Subunits With the Wild-Type α-Subunit

Various combinations of 0.4 μg of wild-type or mutant HADHB-FLAG expression vectors and 0.4 μg of the HADHA-MYC expression vector were co-transfected into HEK293 cells in 24-well dishes using Lipofectamine 2000 reagent (Life Technologies, Carlsbad, CA). Sixty hours after transfection, the cells were collected, and the extracts were subjected to immunoprecipitation using anti-FLAG M2 antibody-conjugated agarose (Sigma–Aldrich) for 2 hr at 4°C with gentle mixing [Yamada et al., 2013]. After washing the gels, the precipitates were subjected to a 10% SDS-PAGE, and proteins were transferred to a PVDF membrane (Immobilon-P). Western blot analysis was performed with anti-FLAG M2 antibody (for the β-subunit) and with anti-MYC antibody (for the α-subunit, kindly provided by Dr. K. Nagata, Aichi Human Service Center). Immunoreactive bands were visualized with an enhanced chemiluminescence western blotting detection system (GE Healthcare, Waukesha, WI).

Structural Analysis of MTP

A homology model of human MTP was built using the Swiss-Model automated modeling server [Kiefer et al., 2009]. N389 and A392 of the β-subunit of the MTP coordinate (PDB code: 1wdk) [Ishikawa et al., 2004] were replaced with aspartate (D) and valine (V), respectively, using the Swiss PDB Viewer [Guex and Peitsch, 1997] to determine the effect of these substitutions on the surrounding residues.

RESULTS

Identification of the Mutation

The nucleotide sequences of all exons and splice sites of the candidate genes of autosomal recessive isolated hypoparathyroidism, *PTH* and *GCMB*, revealed no mutations. Since mutations of *HADHA* and *HADHB* cause rhabdomyolysis in infancy, we determined the nucleotide sequences of all exons and intron-exon boundaries of the genes from the patients and identified a homozygous mutation (c.1175C>T, [p.A392V]) in exon 14 of *HADHB* (NM_000183) (the first methionine is numbered as one) (Fig. 1C). PCR-RFLP analysis demonstrated that the patients were homozygous, whereas the parents and grandmother were heterozygous for the mutation (Fig. 1D). The mutation was absent in 200 normal alleles.

A392V in the β-Subunit Causes MTP Deficiency

The LCKT activities of the lymphoblastoid cells of the Patients IV-1 and IV-2 were decreased to 5% and 14% of normal controls, respectively (Fig. 2A). Western blot analysis showed faint or no bands for the α- and β-subunits bands of MTP from the patient's lymphoblastoid cells. In contrast, both subunits were clearly detected in control lymphoblastoid cells (Fig. 2B). Thus, the patients were found to have MTP deficiency caused by decreased amounts of α- and β-subunits.

The A392V β-Subunit Does Not Associate With the α-Subunit of MTP

Hetero-octamer formation of the four α- and four β-subunits is necessary for MTP activity. To confirm the MTP deficiency evaluated by the enzyme assay and western blot analysis, we studied the effect of mutant β-subunits on the formation of the MTP hetero-octamer with the α-subunit by immunoprecipitation. Western blot

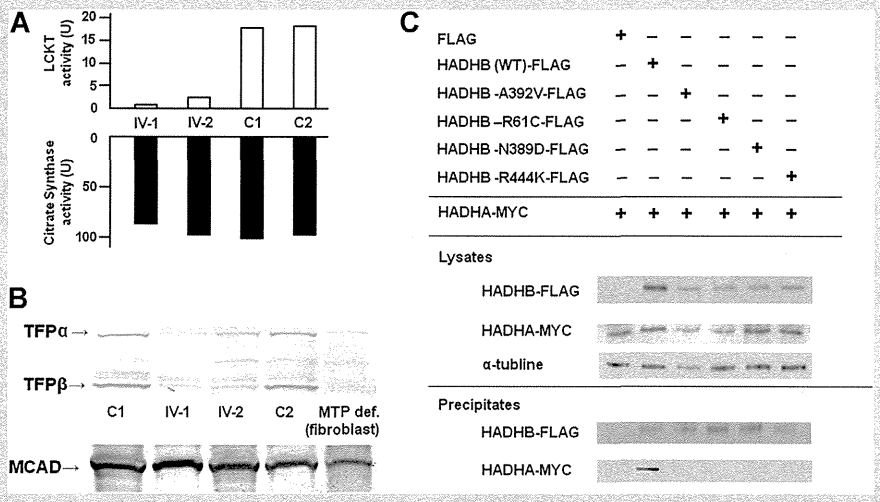

FIG. 2. Biochemical analyses of the MTP protein of the patients. A: The LCKT activities [upper panel] and citrate synthase activities [lower panel] in lymphoblastoid cells from the patients and two controls are shown [1U = μmol/min/mg protein]. B: Western blot analysis of the α- and β-subunits of MTP and MCAD protein [EC 1.3.99.3] [positive control] from the patients and controls lymphoblastoid cells and MTP-deficient fibroblasts are shown. C: Immunoprecipitation of the wild-type or mutant β-subunits with the wild-type α-subunit. [+] Indicates the FLAG- or MYC-tagged vectors used in each study. Lysates and precipitates were immunoblotted with antibodies as indicated [FLAG, MYC, and α-tubulin]. The results of western blot analysis are shown.

analysis revealed that expressions of the mutant β-subunit proteins were decreased in HEK293 cells (Fig. 2C, Lysates), but were efficiently precipitated (Fig. 2C, Precipitates). The MYC-tagged α-subunit co-precipitated with the FLAG-tagged wild-type β-subunit, whereas less than detectable levels of the α-subunit co-precipitated with the four mutant β-subunits (Fig. 2C). Thus, the A392V mutation, as well as the β-subunit N389D mutation previously reported as being associated with a hypoparathyroidism phenotype, abolished the formation of the MTP hetero-octamer, similar to other β-subunit mutations such as R61C (previously described as R28C; lethal phenotype) and R444K (previously described as R411K; neuromyopathic phenotype) [Spiekerkoetter et al., 2003; Purevsuren et al., 2009].

N389D and A392V Mutations Affect the Conformation of the β-Subunit

We analyzed a homology model of the β-subunit of human MTP. N389 and A392 of human MTP are located on the solvent-exposed surface of tetrameric MTP (Fig. 3A). These data indicated that N389 and A392 are not involved in the intersubunit interaction. The catalytic triad, composed of C138, H428, and C458 (shown as blue letters), is located very close to N389 and A392 in the homology model of human MTP (Fig. 3B). Moreover, N389 and A392 are both located on the Cα2 helix in the homology model and directly interact with the Cα1 helix. Notably, the hydrogen bond between the side chains of D389 and T356 is missing in the N389D human MTP model (Fig. 3B,C), and a slight steric clash exists between the side chains of V392 and T356 in the A392V mutant model (Fig. 3D).

DISCUSSION

MTP deficiency caused by mutations of *HADHA* or *HADHB* has been classified into three clinical phenotypes: a lethal phenotype with neonatal onset (severe form), a hepatic phenotype with infantile onset (intermediate form), and a neuromyopathic phenotype with late-adolescent onset (mild form) [Spiekerkoetter et al., 2003]. The clinical features of the patients, together with their decreased LCKT activities, the decreased protein levels of both α- and β-subunits in the patients' lymphoblastoid cells, and the failure of the mutant β-subunit to form an active hetero-octamer with the wild-type α-subunit of the MTP protein indicate that the patients presented in this study have the neuromyopathic phenotype of MTP deficiency due to a homozygous A392V mutation in *HADHB*. Spiekerkoetter et al. [2004] reported that the neuromyopathic phenotype is the major phenotype of MTP deficiency. In contrast, only two of six Japanese cases reported in the literature have presented with the neuromyopathic phenotype [Purevsuren et al., 2009; Yagi et al., 2011]. The fact that the number of cases reported with the neuromyopathic phenotype in Japan is small is most likely because this phenotype is included in the differential diagnosis of early or late-adolescent onset CMT disease with or without episodic myoglobinuria [Spiekerkoetter et al., 2004].

Only two cases of MTP deficiency associated with hypoparathyroidism have been reported (Table I). Dionisi-Vici et al. [1996] first